Geophysical Journal International

Geophys. J. Int. (2013) **195,** 821–843
Advance Access publication 2013 August 8

doi: 10.1093/gji/ggt260

Evidence of Early Cretaceous remagnetization in the Crimean Peninsula: a palaeomagnetic study from Mesozoic rocks in the Crimean and Western Pontides, conjugate margins of the Western Black Sea

Mualla Cengiz Çinku,[1] Z. Mümtaz Hisarli,[1] Naci Orbay,[1] Timur Ustaömer,[2] Ann M. Hirt,[3] Swetlana Kravchenko,[4] Oleg Rusakov[4] and Nurdan Sayın[1]

[1]*Faculty of Engineering, Department of Geophysical Engineering, Istanbul University, Avcılar* 34320*, Istanbul, Turkey. E-mail: mualla@istanbul.edu.tr*
[2]*Faculty of Engineering, Department of Geological Engineering, Istanbul University, Avcılar* 34320*, Istanbul, Turkey*
[3]*Insitut für Geophysics, Sonneggstrasse* 5*, ETH-Zürich,* 8092 *Zurich, Switzerland*
[4]*Institute of Geophysics, National Academy of Sciences of Ukraine (NASU) Kiev, Ukraine*

Accepted 2013 July 2. Received 2013 June 19; in original form 2011 September 30

SUMMARY

We report on a palaeomagnetic study from Mesozoic sedimentary and volcanic rocks from the conjugate areas of the Western Black Sea Basin; that is, the Crimean Peninsula in the north and the Western and Central Pontides in the south, to better constrain their palaeogeographic relationships within the southern margin of Eurasia.

From the study of 87 sites in Crimea, we found that Triassic to Lower Jurassic sandstones and siltstones from the Tavric series, and Middle–Upper Jurassic sandstones, siltstones and limestones exhibit remagnetization. Both fold and conglomerate tests confirm a widespread remagnetization in Crimea. Comparison of palaeopoles with the expected reference apparent polar wander path (APWP) of Eurasia and results from conglomerate tests suggest that the remagnetization occurred in the Early Cretaceous. In the Central Pontides, no reliable palaeomagnetic results can be obtained from Triassic–Upper Jurassic rocks, however, a negative fold test in Upper Jurassic–Lower Cretaceous rocks from the Western Pontides shows that the palaeolatitude agrees with Lower Cretaceous data from Crimea. Our new palaeomagnetic results indicate a pervasive remagnetization in Crimea and the Western Pontides that could be attributed to the rifting phase of the Black Sea Basin during Lower Cretaceous.

Key words: Palaeomagnetism applied to tectonics; Palaeomagnetism applied to geological processes; Remagnetization.

1 INTRODUCTION

The Western Black Sea region comprises a system of Alpine orogenic chains within Turkey to the south and Ukraine to the north. It is surrounded tectonically by the orogenic belts of the Pontides that are subdivided into the İstanbul Fragment, the Istranca and Sakarya zones according to Okay *et al.* (1994), and the Crimean Trough, which belongs to the southern boundary of the Scythian Platform (Saintot *et al.* 2006) (Fig. 1). Due to inconsistent palaeomagnetic data, the Mesozoic palaeopositions of both the Pontides and Crimea are known only partly. Geological and tectonic studies indicate that both the Central Pontides and Crimea show similar stratigraphic successions between Late Triassic and Early Cretaceous, and therefore can be considered to be a single tectonic entity until pre-Cenomanian. After the opening of the Western Black Sea, which led to the formation of a backarc basin during northward consumption of the Izmir–Ankara–Erzincan ocean (northern Neotethys) in the Aptian–Albian, the tectonic environment of the two neighbouring regions changed. Magmatic activity dominated throughout the entire Pontide region during the Upper Cretaceous, whereas marls and carbonates were deposited in Crimea (Letouzey *et al.* 1977; Dercourt *et al.* 1986, 1993; Zonenshain & Le Pichon 1986; Finetti *et al.* 1988; Görür 1988, 1997; Görür *et al.* 1993; Okay *et al.* 1994; Nikishin *et al.* 1996, 1998, 2001; Banks 1997; Ustaömer & Robertson 1997).

Over the last two decades, a number of palaeomagnetic studies have been carried out on the Turkish blocks to better constrain their Mesozoic palaeogeographic evolution. Palaeomagnetic studies from Jurassic rocks in the East Pontides and the NW Sakarya zone place these fragments at a palaeolatitude between ∼30° and 40° during Jurassic–Early Cretaceous (Evans *et al.* 1982; Channell *et al.* 1996; Çinku 2011). The Jurassic palaeogeographic position

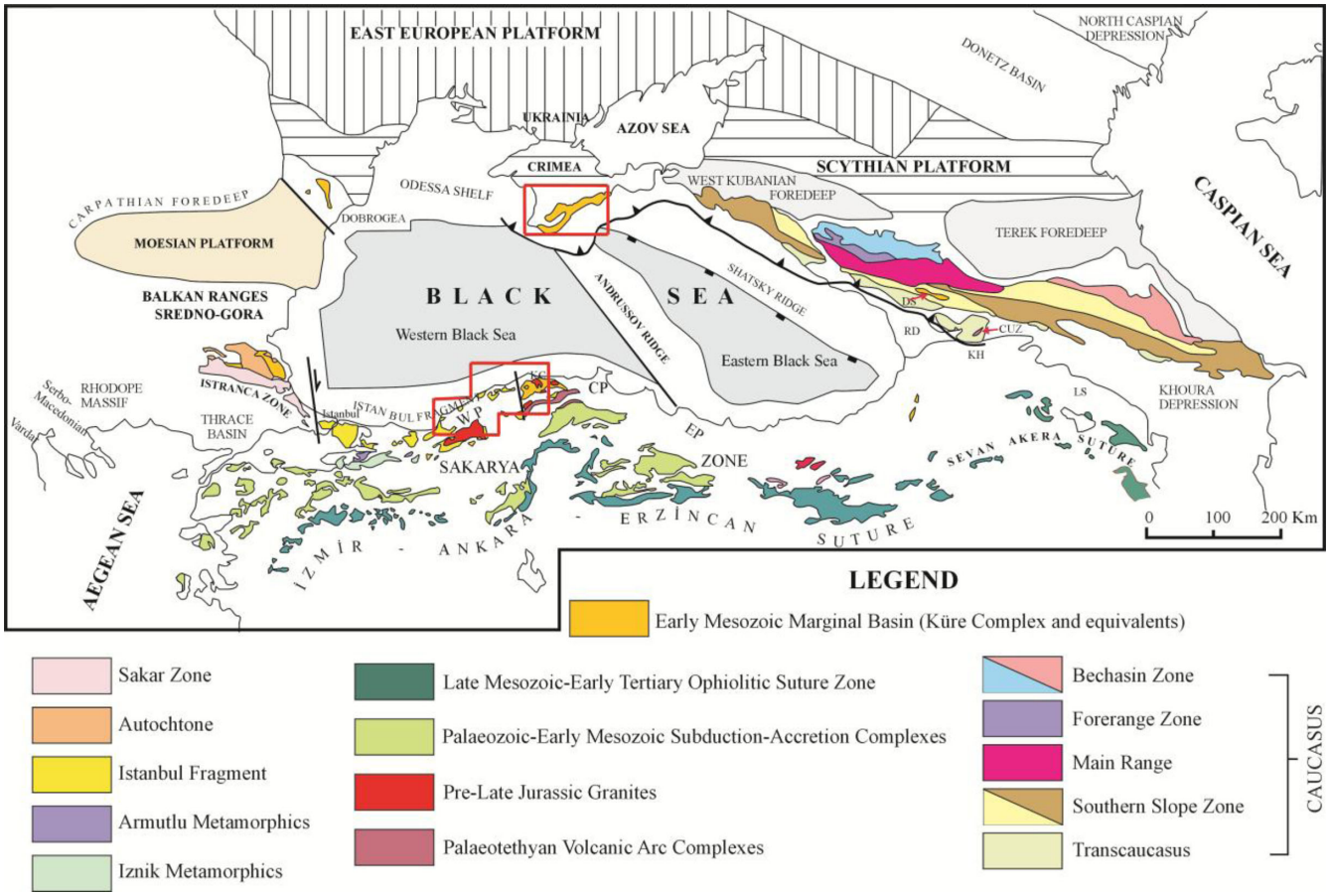

Figure 1. Main tectonic units of the Black Sea region (after Ustaömer & Robertson 2010). Red boxes show the sampling areas. Abbreviations: CUZ, Chortchana–Utslevi unit; DS, Dzirula Salient; KH, Kura High; LS, Loki Salient; RD, Rioni Depression (all in the Caucasus); CP, Central Pontides; EP, Eastern Pontides; IF, Istanbul Fragment; K, Küre Complex; WP, Western Pontides (in N Turkey).

of Crimea, however, is poorly confined by palaeomagnetic data. A study by Meijers *et al.* (2010a) reported that both the Crimea and Western Pontides, migrated from an equatorial position to a palaeolatitude of 30° between Late Jurassic to Cretaceous, synchronous with the Adria terrane. The authors considered the magnetization as primary, based on four sites in Crimea and two sites in the Pontides. They found a palaeolatitude approximately 15° lower than what is predicted by the Eurasian APW path in this time period, and attributed the discrepancy to true polar wander.

To clarify the palaeolatitudianal positions of the present Black Sea region during the Mesozoic, we have carried out a widespread palaeomagnetic investigation on tectonic units from both Crimea and the Western–Central Pontides. The new results help to constrain the age of magnetization and have important implications for the geodynamic evolution of within this region.

2 REGIONAL GEOLOGICAL SETTINGS

Rocks were sampled from opposite margins of the Western Black Sea Basin (Figs 1 and 2a–c). Abundant geological information demonstrates that both the Pontides and Crimea (the conjugate margins of the Western Black Sea Basin) formed a single tectonic domain prior to the opening of the Western Black Sea Basin in the Early Cretaceous (Finetti *et al.* 1988; Görür 1988; Ustaömer & Robertson 1993, 1997; Okay *et al.* 1994; Stephenson & Schellart 2010; Nikishin *et al.* 2011). We briefly summarize the stratigraphy and kinematics of the rock succession in the Western and Central Pontides and the Crimea, examined in this study, in the following subsection.

2.1 The northern margin

The overall shape of the Crimean mountains is the result of subsequent deformation of the Cimmerian and Alpine deformations. The most important deformation stage is defined during the Cimmerian compressional phase (Triassic–Jurassic), with south vergent folding and thrusting (Koronovsky & Mileyev 1974; Khain 1984). The Cimmerian stratigraphy of the Crimean Peninsula starts with the Tavric flysch, which is a highly deformed unit of Triassic–Lower Jurassic siliciclastic turbidites, alternating with shales. Carboniferous limestone blocks are occasionally found in the Tavric flysch. Intense zones of shearing within the unit separate more coherent successions, *ca.* 1000 m thick. The Tavric flysch correlates with the Küre Complex in the Central Pontides (Ustaömer & Robertson 1993, 1994; Robinson & Kerusov 1997; Nikishin *et al.* 2011).

The deformed Tavric flysch is unconformably overlain by the Bitak conglomerates of Mid-Jurassic age, which reflect partial inversion of the Triassic–Liassic flysch basin by the Aalenian (Nikishin *et al.* 2011; Fig. 3c). Arc-type volcanics and intrusions follow statigraphically (Spiridonov *et al.* 1990; Sysolin & Pravikova 2008). Recent radiometric dating of these volcanics indicates an age of *ca.* 165 Ma (Ar–Ar) for magmatic emplacement on the Crimean Peninsula (Meijers *et al.* 2010a).

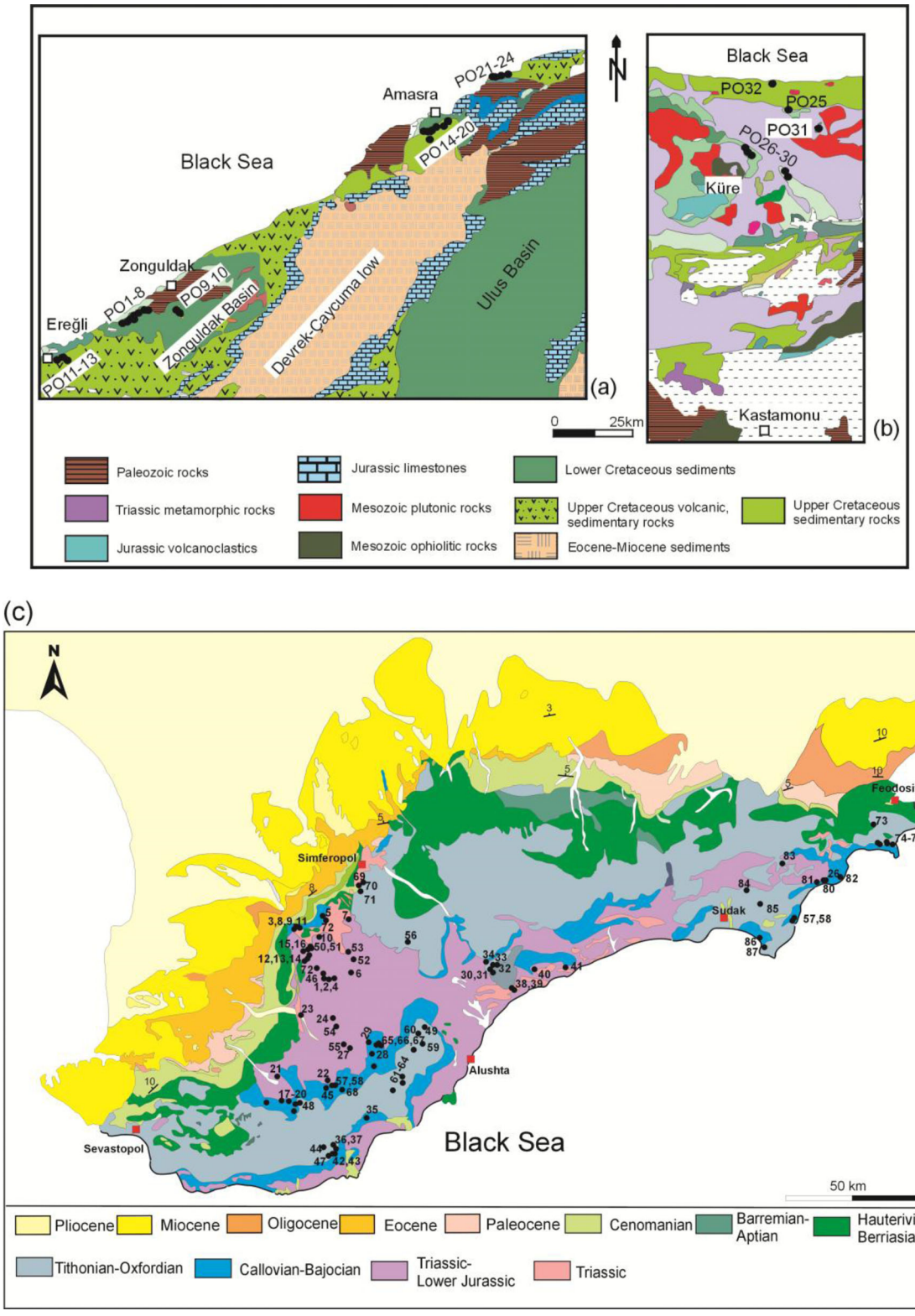

Figure 2. Geological map with numbered sampling site locations for (a) Western (b) Central Pontides and (c) Crimea (Geology map of Crimea modified after Yudin 2000).

Upper Jurassic–Lower Cretaceous units transgressively overlie the older units across a regional unconformity. These cover units have red continental clastics overlain by neritic carbonates. The platform-type carbonates form high mountains with summits trending parallel to the Black Sea coast on the Crimean Peninsula. However, further east in Feodosiya, Upper Jurassic sediments were deposited in a deeper marine basin, filled with turbidites and debris flow deposits (Mileyev *et al.* 1996; Yudin 1999, 2007; Golonka 2004; Arkad'ev *et al.* 2006; Panek *et al.* 2009).

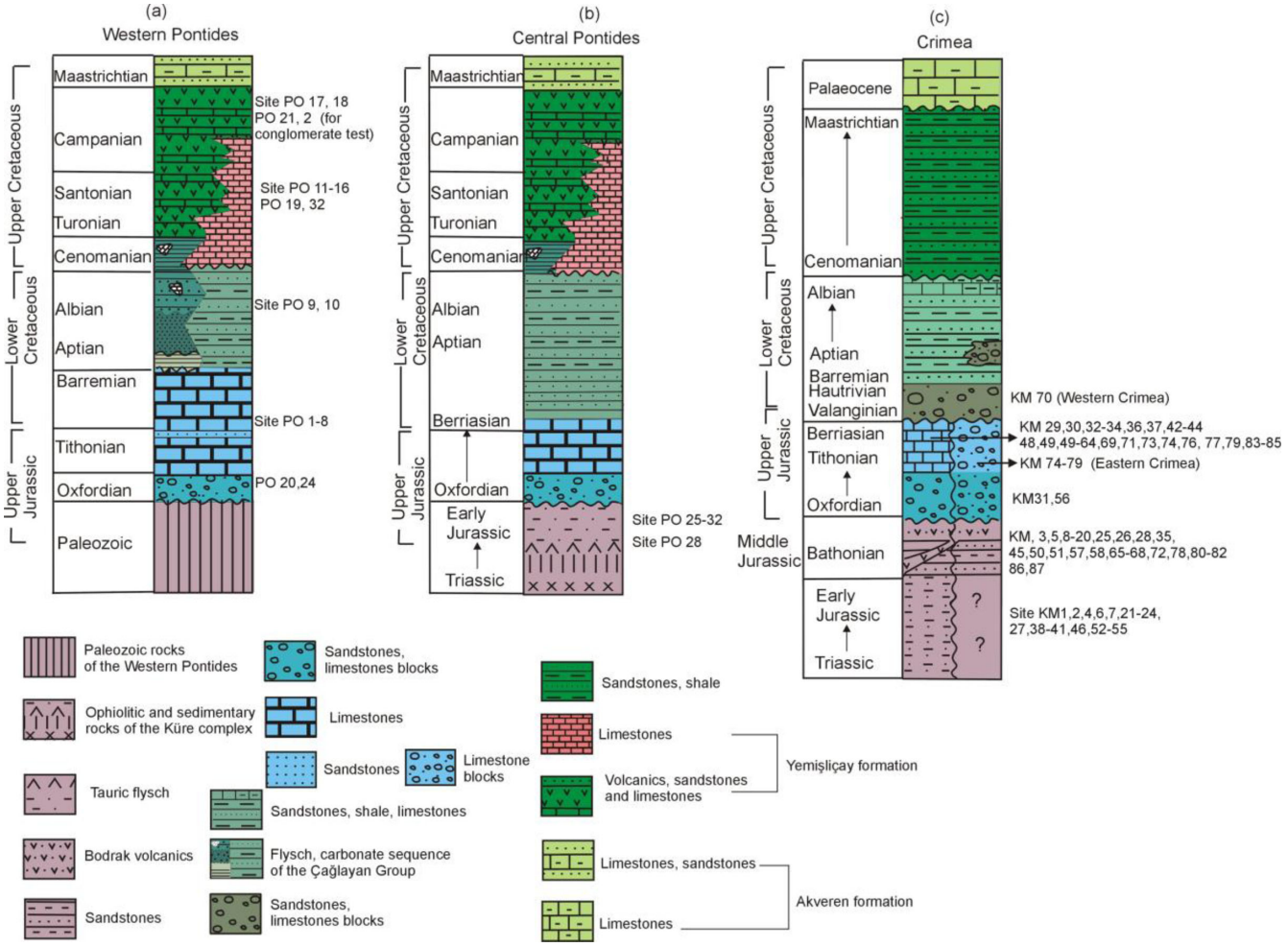

Figure 3. Generalized stratigraphic column section showing the sampling sites in (a) Western Pontides (modified after Görür 1997), (b) Central Pontides (modified after Ustaömer & Robertson 1997) and (c) Crimea (our field study).

The Upper Jurassic–Lower Cretaceous carbonate platform was broken up during an extensional event in the Albian, similar to that recorded on the southern margin. This process was interpreted as the opening of the Black Sea backarc basin due to the northward subduction of the northern branch of the Neotethys (Şengör & Yılmaz 1981; Görür 1988; Okay *et al.* 1994; Banks 1997; Görür & Tüysüz 1997; Ustaömer & Robertson 1997; Nikishin *et al.* 2011). Debris flows, breccia conglomerates and turbidites were deposited in grabens, whereas the limestones were deposited on horsts; Upper Jurassic sediments are not exposed in the north. In this region, Valenginian to Aptian conglomerates, sandstones and shales overlie the Tavric flysch unconformably. The uplift of the Crimean mountains is interpreted to be due to the subduction of the East Black Sea Basin under the Russian Platform (Kazantsev 1982; Slavin 1989; Saintot *et al.* 1999; Nikishin *et al.* 2001; Mileyev *et al.* 2006) with a final uplift in the Middle Pliocene (Lysenko 1976).

2.2 The southern margin

Two tectonic entities are exposed along the southern part of the Western Black Sea Basin. The first of these is the İstanbul Fragment in the Western Pontides and the other is the Küre Complex in the Central Pontides (Fig. 1). The contact between these two units is tectonic (Ustaömer & Robertson 1993, 1994, 1997; Okay *et al.* 1994; Tüysüz 1999; Cavazza *et al.* 2008). An Upper Jurassic–Lower Cretaceous platform-type carbonate and clastic succession forms a common cover over both units.

The İstanbul Fragment comprises a well-developed, uninterrupted, Ordovician to Lower Carboniferous sedimentary succession, representing a passive margin succession facing the Rheic Ocean (Abdüsselamoğlu 1977; Şengör & Yılmaz 1981; Şengör 1984; Ustaömer & Robertson 1993, 1997; Okay *et al.* 2008, 2011; Ustaömer *et al.* 2011). This continental terrane was deformed during the Variscan orogeny in Late Carboniferous time. Rocks from the Permian and Triassic consist of continental sediments in the eastern part (Zonguldak area), and a shallow marine Triassic succession in the west (İstanbul area). A Late Jurassic marine transgression in the Zonguldak area led to the deposition of platform-type carbonates (İnaltı Formation; Şengör *et al.* 1984; Görür *et al.* 1993; Okay *et al.* 1994). The carbonate sedimentation was interrupted shortly before the Barremian by deposition of red conglomerates and sandstones. Carbonate sedimentation was renewed in the Barremian (Zonguldak Formation; Yergök *et al.* 1987a,b), but was completely replaced by a flyschoidal sequence, the Çağlayan Group, in the Aptian. The Çağlayan group is made up of different rock assemblages, composed of dark coloured shales (Figs 2a and 3a; Görür 1997; Tüysüz 1999). These latter are interpreted to be syn-rift deposits of the Western Black Sea. Both the carbonates and the flysch sediments

of the Çağlayan group outcrop extensively in the Zonguldak and Ulus basins (Fig. 2a). Large blocks of Palaeozoic sediments and Upper Jurassic–Lower Cretaceous limestone blocks are found in this flyschoidal sequence. This succession is believed to represent the onset of rifting in the Western Black Sea Basin (Görür *et al.* 1993). This syn-rift succession is unconformably overlain by pink pelagic limestones of the Senomanian–Campanian Kapanboğazı Formation (Görür 1997; Tüysüz *et al.* 2012). Higher up in the stratigraphic sequence, there is a volcanic succession composed of lavas, lava breccias and volcaniclastic turbidites of the Yemişliçay Formation (Fig. 3a). This volcanogenic succession is interpreted as either the production of arc magmatism, occurring during the northward subduction of the Neotethys (i.e. the İzmir–Ankara–Erzincan Suture), or extensional magmatism, related to the opening of the Western Black Sea Basin (Şengör & Yılmaz 1981; Tüysüz *et al.* 1990; Yılmaz *et al.* 1997; Keskin 2003; Keskin *et al.* 2011; Tüysüz *et al.* 2012).

The Central Pontide succession in the east of the İstanbul Fragment is represented by the Triassic–Lower Jurassic Küre Complex, which forms a basement to the Upper Jurassic–Cenozoic succession (Figs 2b and 3b). The Küre Complex is a structurally thickened wedge of siliciclastic turbidites interleaved with tectonic slices and blocks of an ophiolite (Ustaömer & Robertson 1993, 1994). The Küre Complex was intruded by Mid-Jurassic granitoids and deformed by thrusting and folding by the Late Jurassic. The Upper Jurassic–Lower Cretaceous succession lies unconformably on the deformed Küre Complex as in the İstanbul zone. Here, the unconformity is marked by red clastics overlain by platform-type carbonates. An Aptian–Albian flyschoidal sequence with olistoliths of Upper Jurassic–Lower Cretaceous limestone blocks follows and records crustal extension and basin formation (Fig. 3b). This flyschoidal succession is interpreted to comprise syn-rift sediments related to the opening of Western Black Sea Basin. The Upper Cretaceous to Lower Cenozoic succession lies unconformably on the Early Cretaceous syn-rift sediments and is composed of pink pelagic limestones, tuffs and marls.

During the Early Cenozoic, the closure of the northern branches of the Neotethys Ocean and the collision of the Sakarya zone with the Anatolide–Tauride Platform, led to a compressional regime in the entire Pontides. Post-collisional magmatism, produced a large

Photo 1. The Tavrik Complex. (a) Black shale-sandstone alternations locally showing low tilting, (b) in most places it shows large tilting; (c) Sandstones of turbiditic origin showing bouma type-sequences; (d) In local places this is highly deformed. (e) The Tavrik complex with white coloured Upper Cretaceous–Eocene carbonates in the distance. Between these two sequences, the Bodrak volcanics occur as a thin band. (f) The Upper Jurassic limestones.

Photo 2. (a) A view from the red shale, sandstone and pebbles of the Barremian–Aptian Inciğez formation; the upper part consists of bioclastic limestones of Albian age, indicating a recommencement of the platform-type carbonate sedimentation after a short period of tectonic activity. (b) Brownish, medium-thicked abundant quartz and pebbles of the Velibey Sandstone; the sandstones are cross-bedded in places. (c) Red pelagic limestones of the Kapanboğazı Formation with angular discordance of volcanoclastic rocks in the upper parts, showing wide distribution along Ereğli-Zonguldak area. (d) The red pelagic limestones of the Kapanboğazı Formation overlying the Lower Cretaceous flysch (Kilimli, Sapça, Tasmaca formations) with angular discordance. This discordance marks the spreading of the Western Black Sea oceanic basin (Görür & Tüysüz 1997).

belt of E–W trending Eocene volcanics along the Izmir–Ankara–Erzincan Suture Zone (IAESZ) and the Intra Pontide suture (Tüysüz *et al.* 1995; Okay & Satır 2006; Keskin *et al.* 2008). Deformation as a result of N–S compression continued until the Mid-Late Miocene, with the development of thrusting, nappe emplacement and strike-slip faulting (Tüysüz & Dellaloglu 1992; Yılmaz *et al.* 1995). During the Pliocene, Arabia continued to move northwards, leading to the westward extrusion of the Anatolian region. Deformation in this time period is reflected by displacement along the northern and eastern Anatolian Transform faults and their second-order faults (*cf.* Le Pichon & Angelier 1979; Barka 1992; Şengör *et al.* 2005).

3 SAMPLING AND METHODS

Intensive fieldwork was carried out intermittently between 2004 September and 2007 in both Crimea and the Pontides. Sediments that are comprised of sandstones, limestones, shale, marls and volcanic–volcanoclastic rocks were sampled at 87 sites from Crimea and 32 sites from the Western Pontides (Figs 1–3). Samples were collected with a gasoline-powered portable rock drill, and oriented with both sun and magnetic compasses.

In Crimea, a total of 19 sites were sampled from turbidite sandstones (KM1), shale–sandstones (KM2, KM21, KM52, KM54), sandstones (KM4, KM6, KM7, KM22–23, KM27, KM39–41, KM46, KM53, KM55) and limestones (KM24, KM38) from the Triassic–Lower Jurassic Tavric series (Fig. 2c; Photos 1a, b, c and d). Middle Jurassic sandstones, shales and limestones observed in the upper levels of the Tavric series were sampled at 17 sites (KM17–20, KM28, KM35, KM57, KM58, KM65, KM72, KM80, KM81, KM86, KM87) whereas volcanoclastic rock were sampled at two sites (KM25, KM 26). Lavas from the Bodrak series were sampled at 18 sites (KM3, KM5, KM8–16, KM45, KM50, KM51, KM66–68, KM82) in the Bodrak valley (Photo 1e). Upper Jurassic limestones were sampled at 21 sites (KM29, KM30, KM32, KM33, KM34, KM36, KM37, KM42–44, KM47, KM59–64, KM69, KM83–85; Photo 1f), sandstones at one site (KM49) and carbonates at two sites (KM71, KM73). Five sites (KM74, KM76–79) were sampled around Feodosiya from Upper Jurassic–Lower Cretaceous sandstones. Two sites (KM31, KM56) were sampled from Upper Jurassic clasts and another two sites (KM70, KM75) were sampled in conglomerates incorporating pebble-sized limestone clasts of Lower Cretaceous and Upper Jurassic (Figs 1, 2c and 3c).

We have sampled platform-type limestones from the İnaltı Formation (PO1), other limestones (PO3, PO4, PO6, PO8), red sandstones–siltstones (PO5, PO7) and red-wine-beige sandstones (PO2) from the Oxfordian–Barramian Zonguldak and İnciğez formations in the Istanbul zone (Figs 2a and 3a; Photo 2a). Two sites have been sampled in the Velibey Formation of Albian age (PO9, PO10) from yellowish–brownish sandstones, which are less deformed and show regular bedding (Photo 2b). Five sites (PO11–PO13, PO19, PO32) were sampled from pink-coloured, pelagic limestones, and three other sites were sampled from volcanoclastics and sandstones (PO14–PO16) of the Kapanboğazı Formation (Photos 2c and d, respectively). Around Kurucaşile, two sites were sampled from volcanoclastic rocks in the Yemişliçay Formation of Campanian age (PO17, PO18) and three sites (PO20, PO23, PO24) were sampled from Upper Jurassic–Lower Cretaceous limestones in the İnaltı Formation. In the same area, a Campanian volcanic debris flow, composed of a ~5-m thick debris flow, composed of deformed

siltstone blocks and large volcanic blocks, is used for a conglomerate test. Other sampling sites comprise volcanic units (PO21, PO22), Küre Complex Liassic turbidites (PO25), flysh (PO26), limestones (PO31) and pillow lavas (PO28). A regional fold test has been carried out on a syncline from the Liassic flysch (PO27, PO29 and PO30) (Figs 1, 2b and 3b).

Cores were cut into standard 2.2-cm long cylindrical specimens and between 7 and 21 palaeomagnetic specimens from each site were subjected to both stepwise thermal and alternating-field (AF) demagnetization. All measurements were carried out at the Laboratory for Natural Magnetism of the ETH-Zürich. Directions and intensities of the natural remanent magnetization (NRM) were measured with a 2G Enterprises 755R three-axes DC-SQUID cryogenic magnetometer. Thermal demagnetization was conducted using an ASC TD48, MTD-80 furnace in progressive steps between room temperature and 680 °C, and AF demagnetization was performed with a 2G-Enterprises degausser attached to the magnetometer between 0 and 100 mT.

NRM directions of representative samples are shown as orthogonal projections during thermal and AF demagnetization (Zijderveld 1967) in Fig. 7; principal component analysis was used to define vector components (Kirschvink 1980). The average ChRM for the sites and corresponding Fisher statistical parameters (Fisher 1953) are given in Table 1.

Detailed rock magnetic experiments, including thermomagnetic measurements, acquisition of isothermal remanent magnetization (IRM), thermal demagnetization of three-axes composite IRM (Lowrie 1990) and hysteresis measurements (Day *et al.* 1977;

Table 1. Palaeomagnetic results for Triassic to Lower Cretaceous samples from Crimea and Lower–Upper Cretaceous samples from the Western Pontides (N = number of samples per locality, n = number of samples used for site mean calculation. α_{95} is the 95 per cent confidence circle, k is the precision parameter (Fisher 1953). Declination $D_{g(s)}$ and inclination $I_{g(s)}$ describe the mean directions in geographic (before tilt correction) and stratigraphic coordinates (after tilt correction), respectively. Lat. (latitude), Long. (longitude) of the sites. *Site which were not considered for tectonic interpretation for reasons given in the text.

Site	Lithology	Lat.(°N)	Long.(°E)	Strike/dip	N/n	D_g	I_g	D_s	I_s	α_{95}	k
				Crimea							
				Triassic–Lower Jurassic (200–175 Ma) sites							
KM1	Turbidite sandstone	44.45.838	34.01.559	150/89	8/6	357.5	40.3	287.3	21.4	11.6	22.5
KM2*	Shale-Sandstone	44.45.481	34.02.255	147/86	8/7	347.1	15.3	312.2	20.3	5.0	14.5
KM4*	Sandstone	44.45.481	34.02.255								
KM6	Sandstone	44.56.704	34.06.094	125/86	9/8	337.3	32.1	270.3	29.3	14.1	16
KM7*	Sandstone	44.57.832	34.00.994	190/89	5/5	256.6	58.3	266.7	−28.4	54.0	2.9
KM21*	Shale-Sandstone	44.35.766	30.00.823	252/20	4/4	3.3	21.2	2.8	2.3	33.0	8.7
KM22	Sandstone	44.35.036	34.03.260	220/24	10/8	11.5	45.2	356.0	30.4	11.3	27.1
KM23	Sandstone	44.41.917	33.58.237								
KM27	Sandstone	44.38.346	34.07.623	343/78	8/6	358.5	64.2	48.5	4.4	3.9	378.1
KM38	Sandstone	44.44.422	34.28.763	231/33	9/7	344.3	45.3	338.4	14.2	12.5	38.2
KM39	Sandstone	44.44.782	34.28.271	126/50	10/6	353.3	35.0	300.8	56.3	10.5	41.4
KM40	Sandstone	44.46.957	34.31.171	213/43	10/9	344.5	69.0	319.2	30.5	8.5	37.6
KM41	Sandstone	44.46.513	34.36.147	277/48	6/6	354.4	43.2	358.1	−4.8	11.5	35.2
KM46	Sandstone	44.45.232	34.03.076								
KM52	Shale-Sandstone	44.46.940	34.06.341	332/74	8/7	310.2	51.8	22.5	27.2	10.5	38.2
KM53	Sandstone	44.47.820	34.05.861	266/86	7/7	345.5	44.3	346.1	−41.6	12.1	25.8
KM54	Black shale sandstone	44.38.693	34.05.171	343/17	9/9	28.5	57.4	41.0	44.4	7.8	44.8
KM55	Sandstone	44.38.302	34.06.117	230/34	9/6	3.6	67.5	340.2	37.4	8.7	202.0
Mean					18/12	351.3	50.7			9.3	22.6
								353.3	27.3	27.6	3.4
				Crimea							
				Middle Jurassic (171–165 Ma) sites							
KM17	Limestone	44.32.830	33.57.532	211/29	7/6	349.3	56.5	331.3	33.5	10.4	23.0
KM18	Sandstone	44.31.082	33.59.071	183/29	8/8	346.5	72.9	302.3	52.3	16.5	12.0
KM19	Sandstone	44.30.902	33.59.262	359/29	9/9	352.1	63.0	39.4	54.9	10.2	35.0
KM20	Sandstone	44.29.436	33.59.679	232/70	9/7	356.0	63.3	337.3	−3.8	11.9	19.7
KM25*	Volcano-clastic	44.33.986	31.19.145	258/33	6/6	52.0	64.2	19.6	40.4	16.0	18.5
KM26	Volcano-clastic	44.54.800	35.12.557	80/74	9/9	345.3	51.0	176.4	55.4	5.8	79.7
KM28	Sandstone	44.37.738	34.08.773	335/34	17/16	20.7	59.2	40.5	30.4	7.8	34.8
KM35	Sandstone	44.30.085	33.59.328	170/28	17/16	19.2	53.6	337.3	57.4	5.1	53.0
KM57	Shale	44.52.793	34.08.196	250/31	7/5	18.0	44.4	8.3	18.2	13.5	33.0
KM58	Shale	44.52.962	34.08.193	311/32	9/8	177.2	−45.4	190.6	−19.9	11.6	44.0
KM65*	Limestone	44.54.042	34.08.859	250/76	6/6	18.4	−12.1	71.4	−53.3	9.8	47.8
KM72	Sandstone	44.46.019	34.01.676	144/85	21/19	2.0	63.7	256.4	21.1	4.7	49.7
KM80	Limestone	44.54.746	35.12.797	259/81	9/8	26.3	37.7	24.2	−32.3	7.5	151.0
KM81	Limestone	44.54.993	35.11.329	58/80	7/6	348.2	58.5	134.1	39.2	9.4	51.7
KM86	Turbidites	44.48.846	35.05.000	316/11	14/9	353.2	31.6	348.2	40.1	11.1	22.5
KM87*	Limestone	44.48.183	35.04.745								
Mean					16/13	2.1	52.9			7.6	31.1
								349.2	19.2	30.9	2.8

Table 1. (*Continued.*)

Site	Lithology	Lat.(°N)	Long.(°E)	Strike/dip	*N*/*n*	D_g	I_g	D_s	I_s	α_{95}	*k*
				Crimea							
				Middle Jurassic (171–165 Ma) sites/Bodrak Volcanics							
KM3*	Volcanic	44.45.481	34.02.255								
KM5*	Volcanic	44.51.133	34.01.904								
KM8	Volcanic	44.49.391	34.02.840	226/78	8/8	7.3	59.0	340.2	−8.5	11.5	24.0
KM9	Volcanic	44.49.391	34.02.840	226/77	8/5	320.1	54.4	319.7	−23.2	12.4	38.0
KM10*	Volcanic	44.49.391	34.02.840								
KM11	Volcanic	44.49.358	34.02.772	227/77	6/5	345.3	28.2	350.1	−41.0	16.0	18.0
KM12*	Volcanic	44.47.094	33.59.443								
KM13*	Volcanic	44.47.108	33.59.357								
KM14*	Volcanic	44.47.128	34.00.212								
KM15	Volcanic	44.47.131	34.00.096	250/41	6/6	311.0	−25.2	286.3	−57.5	15.0	20.0
KM16	Volcanic	44.47.965	33.59.510	124/82	12/10	2.3	70.3	225.3	25.4	12.4	16.0
KM45	Volcanic	44.45.232	34.03.076	328/4	8/7	42.4	27.0	43.8	23.6	12.7	23.6
KM50*	Volcanic	44.49.436	34.02.836								
KM51*	Volcanic	44.49.436	34.02.836								
KM66*	Volcanic	44.54.042	34.08.859	246/74	5/5	7.9	22.1	15.1	−41.2	42.0	4.3
KM67*	Volcanic	44.54.042	34.08.859								
KM68*	Volcanic	44.54.057	34.08.601	243/77	5/5	56.7	−12.4	73.5	−9.5	31.0	7.0
KM82*	Volcanic	44.55.818	35.14.312								
Mean					18/6	349.7	41.8			40.2	3.7
								355.4	−28	46.3	3.0
				Crimea							
				Upper Jurassic (160–145 Ma) sites							
KM29	Limestone	44.36.559	34.09.530	163/12	8/8	11.3	62.7	347.2	65.6	7.0	63
KM30*	Limestone	44.45.757	34.23.442	209/26	6/4	6.5	68.5	331.7	50.3	19.0	26
KM33	Limestone	44.46.841	34.25.203	238/45	12/12	10.4	71.3	343.0	30.9	9.0	24.0
KM34*	Limestone	44.47.172	34.25.354	213/41	4/3	345.6	60.1	325.1	24.2	12.0	100
KM36	Limestone	44.29.053	34.02.749	239/22	10/7	358.2	56.4	349.5	36.5	9.4	42
KM37*	Limestone	44.28.778	34.02.369	236/19	5/5	160.3	−7.4	160.2	11.4	9.7	62
KM42	Limestone	44.28.296	34.04.573	125/20	7/6	344.0	22.0	335.4	33.3	8.6	62
KM43	Limestone	44.28.296	34.04.573	123/20	7/7	348.9	38.4	332.4	50.4	8.3	45
KM44*	Limestone	44.28.143	34.04.224	172/59	9/9	330.3	58.3	292.2	15.5	28.0	4.0
KM47*	Limestone	44.45.606	34.00.182	335/4	13/13	151.0	−11.2	151.8	−11.3	10.0	19
KM48*	Limestone	44.46.795	34.01.887	250/13	5/5	347.7	51.3	346.3	38.3	46.0	3
KM59	Limestone	44.40.559	34.16.582	197/46	8/8	4.4	48.7	333.8	24.2	8.2	47
KM60	Clayey limestone	44.39.745	34.15.670	211/65	18/18	21.1	62.7	330.6	18.6	4.0	75
KM61	Clayey limestone	44.38.298	34.15.127	208/34	14/14	45.7	53.4	0.4	49.5	4.4	81
KM62*	Clayey limestone	44.36.917	34.13.645	245/45	6/3	4.5	55.3	352.0	13.5	31.0	16
KM63*	Limestone	44.35.040	34.13.780	176/37	10/5	350.1	39.1	326.2	27.6	17.0	21.2
KM64	Limestone	44.34.372	34.12.269	160/29	9/7	348.3	65.2	297.5	55.1	6.0	89.5
KM71*	Carbonate	44.54.035	34.08.455								
KM73	Carbonate	45.00.549	35.19.636	272/34	15/15	344.6	64.6	353.1	31.2	6.0	12.5
KM83	Limestone	44.56.086	35.09.090	293/20	16/13	8.4	56.7	13.5	36.2	5.5	58.5
KM84	Limestone	44.53.798	35.02.330	305/82	7/7	3.5	45.4	10.4	−29.7	7.0	71.7
KM85	Limestone	44.52.518	35.03.560	251/33	8/14	7.6	49.3	359.3	18.6	8.0	27.9
Mean					23/14	0.5	52.9			6.1	31.1
								356.2	43.5	22.4	3.9
				Crimea–Feodosiya area							
				Upper Jurassic–Lower Cretaceous (145–130 Ma) sites							
KM74	Sandstone	44.57.695	35.21.342	44/33	14/13	341.2	52.0	37.7	73.7	8.0	30
KM76	Sandstone	44.57.695	35.21.342	42/45	17/16	356.2	55.2	78.8	61.2	5.0	47
KM77	Sandstone	44.57.395	35.21.778	43/45	20/20	358.2	59.3	87.0	60.3	5.8	32
KM78	Sandstone	44.58.083	35.17.312	78/51	15/10	23.7	32.5	75.5	60.8	5.3	86
KM79	Sandstone	44.58.072	35.17.459	47/44	9/9	5.4	46.2	65.4	57.5	11.0	23
Mean					5/5	2.4	49.7			14.2	29.9
								71.4	63.1	9.3	68.1
				Conglomerate test							
KM31	Limestone cobbles	44.45.994	34.24.630	234/37	11/6	359.2	63.3	341.4	29.1	12.8	15.2
KM56	Limestone cobbles	44.48.797	34.14.073	230/31	10/10	12.7	69.9	342.9	43.4	12.3	18.5
KM70	Limestone cobbles	44.54.035	34.08.455	58/15	6/6	340.2	−70.2	335.2	−55.2	50.0	1.9
KM75	Limestone cobble	44.57.695	35.21.342	62/4	7/7	344.3	66.7	346.2	69.9	47.4	2.0

Table 1. (*Continued.*)

Site	Lithology	Lat.(°N)	Long.(°E)	Strike/dip	*N*/*n*	D_g	I_g	D_s	I_s	α_{95}	*k*
				Pontides							
				Triassic/Lower Jurassic (200–175 Ma) sites							
PO25	Turbidite	41.55.339	33.44.201	237/81	6/6	159.7	70.1	322.5	29.8	25.1	21
PO26	Flysch	41.53.768	33.42.354	21/45	6/5	33.6	68.2	84.7	37.8	27	12
PO27*	Flysch	41.53.768	33.42.354								
PO28*	Pillow lava	41.48.742	33.42.970								
PO29*	Flysch	41.47.142	34.05.085								
PO30*	Flysch	41.47.142	34.05.085								
PO31*	Limestone	41.45.689	34.02.020	135/3	6/6	324.3	13.0	323.2	13.9	23.0	27.0
				Pontides							
				Upper Jurassic–Lower Cretaceous (145–120 Ma) sites							
PO1	Limestone	41.26.072	31.26.072	43/27	15/9	331.3	39.1	345.8	63.7	8.4	28.5
PO2	Sandstone	41.25.327	31.43.205	236/48	9/9	357.1	61.3	341.1	16.2	11.0	23.7
PO3	Limestone	41.24.803	31.43.001	139/38	7/5	338.4	51.1	291.2	47.6	11.1	18.6
PO4	Sandstone	41.25.395	31.43.372	247/44	8/6	311.2	65.1	325.4	22.8	10.4	22.3
PO5	Sandstone-Siltstone	41.25.689	31.43.020	110/55	8/7	330.0	43.1	262.7	50.9	7.0	56.2
PO6	Limestone	41.25.658	31.43.593	218/43	9/9	355.2	43.4	340.8	9.1	6.2	52.3
PO7	Sandstone	41.27.117	31.45.519	289/39	9/7	322.3	54.3	346.3	25.1	7.2	72
PO8	Limestone	41.27.134	31.45.522	257/39	7/5	23.1	55.3	8.2	20.2	8.0	58
Mean					9/8	161.0	−53.3		11.1		
								152.5	−35.6	23.5	6.5
				Pontides							
				Upper Cretaceous (83–70 Ma) sites							
PO9*	Sandstone										
PO10*	Sandstone	41.25.868	31.52.819	80/24	8/7	354.3	39.3	357.0	63.4	22	13
PO11	Pelagic limestone	41.19.088	31.33.099	88/11	8/8	308.6	43.7	299.4	49.3	12.6	20.1
PO12	Limestone	41.19.030	31.32.740	31/5	7/7	326.6	28.5	327.6	33.6	9.1	45.0
PO13	Limestone	41.16.440	31.29.425	123/10	7/7	325.3	25.7	320.0	28.6	7.0	76.0
PO14	Pelagic limestone	41.44.181	32.24.654	38/41	4/4	322.4	14.2	331.5	53.5	6.8	182.0
PO15*	Sandstone										
PO16*	Sandstone										
PO17*	Volcano-clastic	41.42.374	32.23.470	9/17	4/4	200.4	−62.3	226.3	−55.5	7.4	153
PO18	Volcano-clastic	41.43.135	32.23.822	59/29	8/6	333.5	27.0	335.9	56.6	10.7	40.0
PO19	Pelagic limestone	41.44.262	32.25.654	87/17	11/11	328.4	38.4	318.3	52.3	4.7	96
PO20*	Limestone										
PO23*	Limestone	41.49.590	32.28.260	244/42	9/9	227.4	−78.0	170.1	−43.0	19.0	7.1
PO32	Limestone	41.56.738	33.45.555	279/44	8/8	250.9	67.0	335.4	53.3	5.8	91.0
Mean					9/7	320.0	36.0			18.5	11.5
								324.1	47.0	11.7	27.4
				Conglomerate test							
PO21	Volcanic cobble	41.49.590	32.28.260	287/31	10/10	325.4	17.8	335.6	14.6	46.7	2.0
PO22	Volcanic cobble	41.49.590	32.28.260	288/31	9/9	263.8	8.2	327.0	18.9	45.4	2.2

Dunlop 2002), were conducted on typical lithologies from the investigated areas. Thermomagnetic experiments were measured on representative samples by heating in air, using an AGICO KLY-2 Kappabridge susceptibility bridge fitted with a CS-2 oven unit. The change in susceptibility is in relative units during the thermomagnetic measurements (i.e. not corrected for the sample holder, although the measurements were normalized for sample mass).

Stepwise acquisition of IRM was made with an ASC pulse magnetizer (Model IM-10-30) up to 1 T along the sample Z-axis (hard component). Afterwards 0.4 T (medium component) was applied to the sample *Y*-axis and 0.12 T (soft component) to the sample *X*-axis (Lowrie 1990). Subsequently, samples were thermally demagnetized to identify the magnetic carriers based on their coercivity and unblocking behaviour. Hysteresis loops were measured on 21 specimens of Crimea and nine specimens from the Pontides, up to a maximum field of 1 T using a Princeton Measurements Corporation MicroMag magnetometer (Model 3900).

4 RESULTS

4.1 Magnetic mineralogy

Thermomagnetic measurements of most samples show a strong decrease in susceptibility between 500 and 600 °C typical of Ti-poor magnetite (Figs 4a, b, d and e). The susceptibility upon cooling is lower in many samples, suggesting some degree of oxidation of magnetite to haematite (Figs 4b, d and f). In a few limestone samples (site KM38, Fig. 4c), the heating curves shows a rapid decrease between 400 and 500 °C, suggesting the presence of titanium-rich magnetite. In some sandstone samples (site KM72), there is a drop

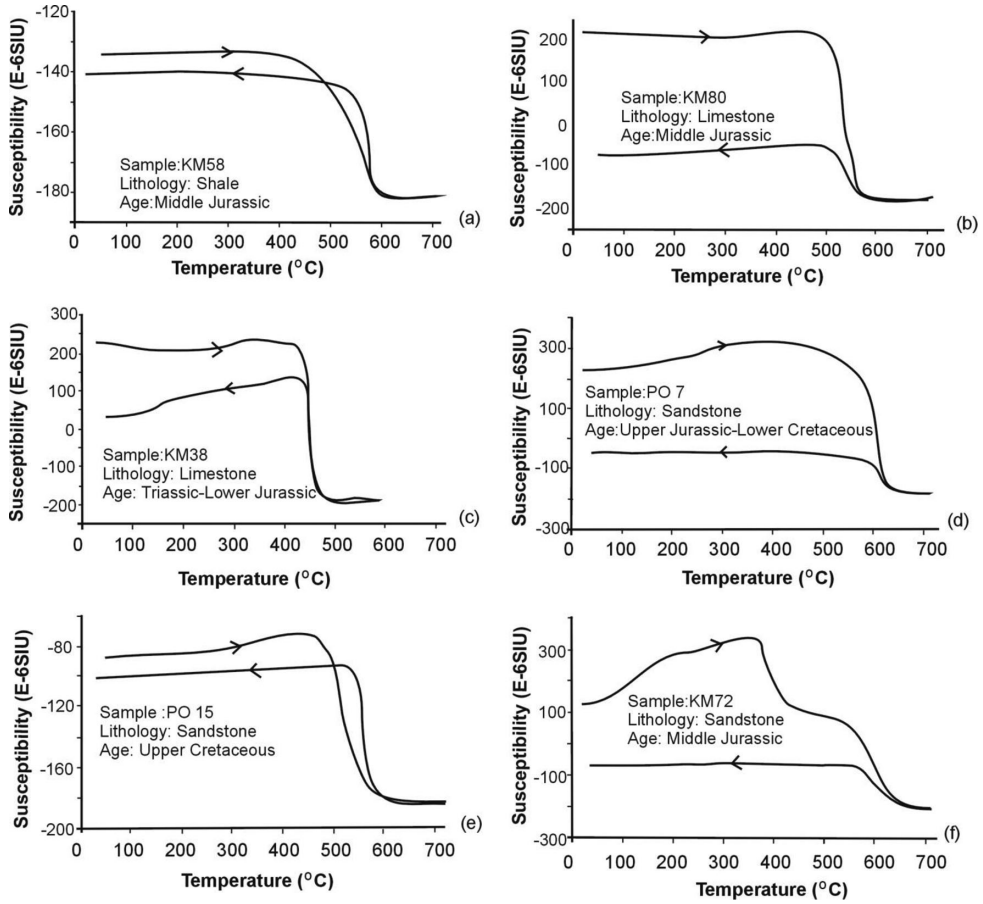

Figure 4. Typical Curie curves for representative samples. Reversible thermomagnetic curve of sample KM58 and PO15 show only one magnetic phase with a Curie temperature around 580 °C (a and e). In contrast, samples (b), (c), (d) and (f) show large amounts of alteration upon heating. Sample KM38 shows a Curie point at 450 °C with some mineralogical alteration upon heating (c). Sample PO7, KM70 shows Curie temperatures above 600 °C, indicative of the presence of titanohaematite (d, f), whereas samples as shown in (f) indicate a drop about 400 °C showing the presence of titanium-rich magnetite.

between 350 and 400 °C, with a final loss of susceptibility at about 650 °C. The loss in magnetization upon cooling suggests that titanomaghemite or titanomagnetite has transformed to haematite (Fig. 4f).

IRM curves show rapid acquisition of magnetization to about 200 mT in general, suggesting the existence of a soft coercivity component (Fig. 5a). Thermal demagnetization of the cross-component IRM shows that the low-coercivity component is gradually unblocked to under 600 °C, and is therefore Ti-poor magnetite (Fig. 5b). Some samples, however are not saturated by 200 mT, indicating the presence of a second magnetic phase with higher coercivity (e.g. KM64.8a, Fig. 5c). Thermal demagnetization, however, shows that a significant part of the high coercivity component is still left at 600 °C, which suggests the presence of haematite. In many cases, the intermediate coercivity (between 0.12 and 0.40 T) is the second strongest component of the IRM (Figs 5d–e). A small drop at 350–400 °C that is seen in some samples (e.g. KM64.8a and KM41.3a; Figs 5c and d) may indicate the presence of a titanium-rich magnetite or maghemite. An unblocking temperature at about 450 °C, in sample PO3.5a, indicates the presence of titanium-rich magnetite (Fig. 5e). From the hysteresis measurements, the ratio of saturation remanence versus saturation magnetization (J_{rs}/J_s) of about 0.01–0.63 and coercivity of remanence versus coercivity ratios (H_{cr}/H_c) of about 0.35–5.24 suggests that most samples have a grain size of pseudo-single domain (PSD; Fig. 6) (Day *et al.* 1977; Dunlop 2002).

4.2 Palaeomagnetism

4.2.1 Crimea

The NRM intensity of the limestone samples ranges between ~0.1 and ~1.1 mA m^{-1} and the sandstone samples between 1 and 30 mA m^{-1}; the volcanic and volcanoclastic rocks lie between 50 and 2000 mA m^{-1}. From a total of 87 sites in Crimea, 58 per cent of the total shows a stable component of magnetization. Six sites from sandstones and limestones of Triassic–Early Jurassic age; 16 sites from the Middle Jurassic Bodrak volcanics; three sites from Middle Jurassic limestones and cherts and eight sites from Upper Jurassic limestones, sandstones and shale/marls were rejected (Table 1) due either to (1) their weak NRM (<0.001 mA m^{-1}), (2) site mean with large α_{95}, (3) unstable behaviours during demagnetization or (4) a large discrepancy from the rest of their group data, for example, KM2, KM37 and KM47. The Q index of Van der Voo (1990), which requires sufficient number of samples ($N \geq 24$, $k > 10$, $\alpha_{95} < 16^\circ$) could not be satisfied at most sites. However, the statistical parameters ($\alpha_{95} \sim 18^\circ$ and $k \sim 10$) for $N = 8$ samples is fulfilled in most of our sample sites.

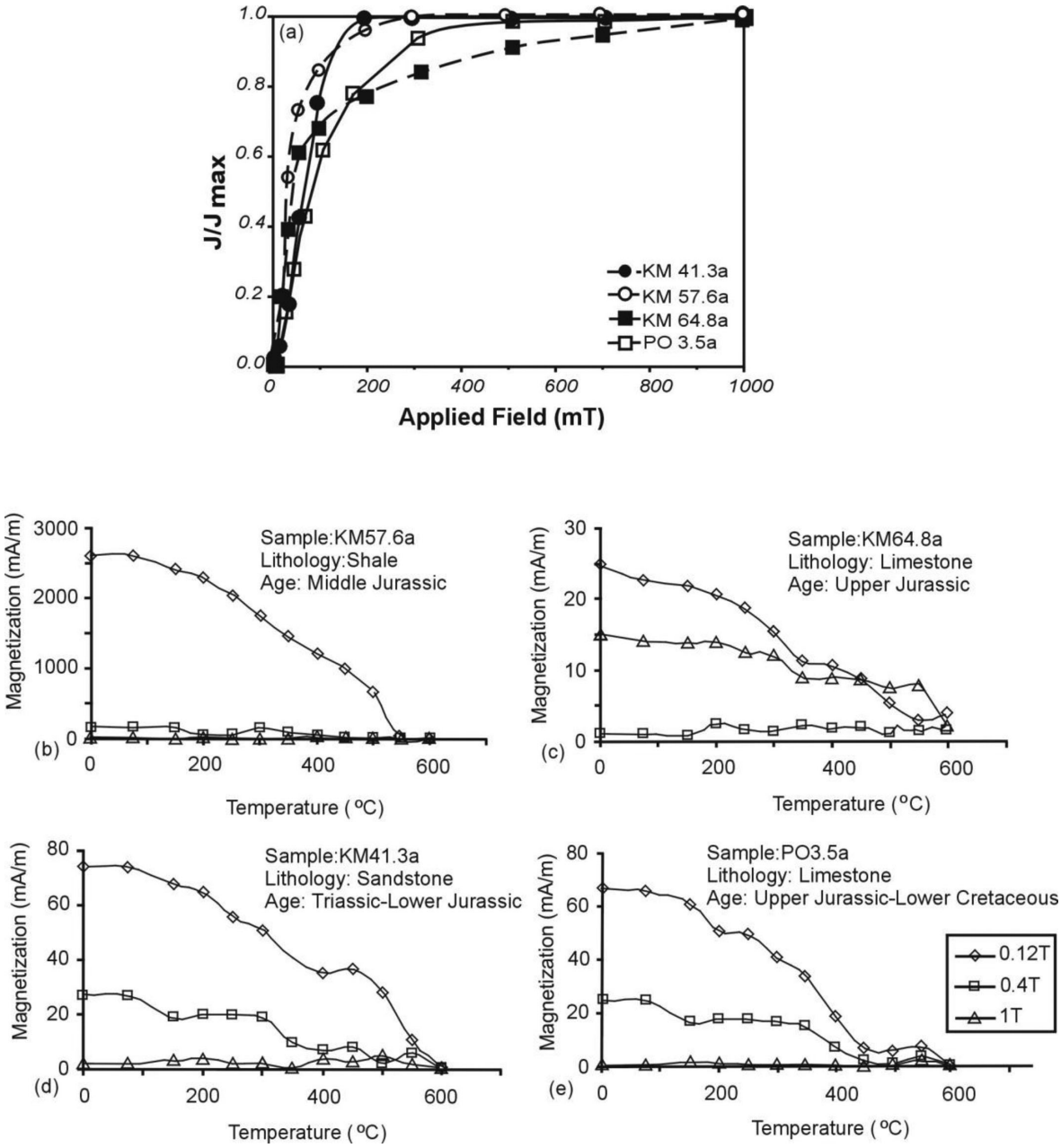

Figure 5. (a) Normalized IRM acquisition curves showing the presence of low-coercivity minerals. (b–e) Thermal demagnetization of three-axis IRM in representative samples. The hard (1 T along the sample *Z*-axis), medium (0.4 along the sample *Y*-axis) and soft (0.12 T along the sample *X*-axis) components are shown as a function of demagnetization temperature.

Usually two NRM components can be isolated during demagnetization (Fig. 7). A low unblocking temperature/low-coercivity component, recording probably a minor viscous origin, is removed between 75 and 100 °C or 5–15 mT, respectively (Figs 7c, d, e, h and i). Several directions of this component are scattered, although in some samples, a direction close to the present Earth's magnetic field (PEF) is presented (Fig. 7f). After removal of this weak overprint, a ChRM direction was calculated from the vector that decays linearly to the origin of the orthogonal vector plots. Most samples have maximum unblocking temperatures between 500 and 580 °C or median destructive fields of 10–40 mT consistent with SD-PSD magnetite as the carrier of the NRM (Figs 7b, c, e, f–i). Several samples, however unblock between 300 and 450 °C, which may indicate the presence of titanium-rich magnetite or maghemite (Figs 7d and e).

The ChRM site mean directions obtained from the sedimentary rocks in Crimea may be grouped into several time periods (i.e. Triassic–Lower Jurassic, Middle Jurassic and Upper Jurassic). All show normal polarity with *in situ* component directions well clustered while directions after tilt correction become more scattered (Table 1, Fig. 8). The ChRM direction obtained from Triassic–Lower Jurassic (CTrLJ) rocks in Crimea is $D/I = 351.3°/50.7°$ ($k = 22.6$, $\alpha_{95} = 9.3°$) before tilt correction and $D/I = 353.3°/27.3°$ ($k = 3.4$, $\alpha_{95} = 27.6°$) after tilt correction (Table 1, Fig. 8a). The Middle Jurassic (CMJ) and Upper Jurassic (CUJ) rocks show a mean direction of $D/I = 2.1°/54.4°$ ($k = 31.1$, $\alpha_{95} = 7.6°$) and

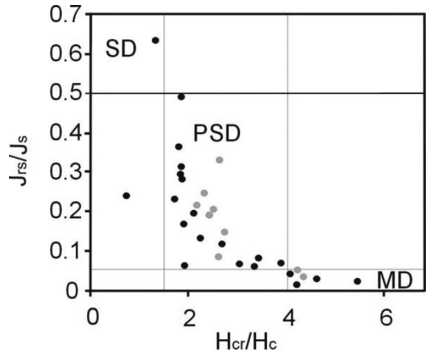

Figure 6. Measured hysteresis ratios plotted on the Day plot (Day *et al.* 1977). Black and grey circles for samples in Crimea and Pontides, respectively; SD, single domain; PSD, pseudo-single domain; MD, multidomain.

$D/I = 0.5^\circ/52.9^\circ$ ($k = 31.1$, $\alpha_{95} = 6.1^\circ$), respectively, before tilt correction and $D/I = 349.2^\circ/19.2^\circ$ ($k = 2.8$, $\alpha_{95} = 30.9^\circ$) and $D/I = 356.2^\circ/43.5^\circ$ ($k = 3.9$, $\alpha_{95} = 22.4^\circ$, respectively, after tilt correction (Table 1, Figs 8b and c).

From the 18 sites collected from the Middle Jurassic Bodrak volcanics, only six (KM8, KM9, KM11, KM15, KM16 and KM45) show stable behaviour during demagnetization, the remainder of the sites were rejected due to unstable behaviour during demagnetization or large scatter between individual sample directions within a site, that is, high α_{95} of 31° and 42° (KM66 and KM68). The mean direction of these rock suits shows a large scatter before and after tilt corrections (Table 1).

Palaeomagnetic fold tests associated with progressive unfolding were applied to the individual groups of different age intervals. All palaeomagnetic groups in Crimea carry a post-folding remanent magnetization. This result is verified by incremental fold test regardless whether McElhinny (1964), McFadden (1990) and Watson & Enkin (1993). The fold test of Watson & Enkin (1993) indicates an optimum degree of untilting at 9.7, with 95 per cent confidence limits at 12.4 and 6.6 per cent for each age intervals (Fig. 9).

The results from two conglomerate tests provide further information on the timing of magnetization. Samples from sites KM31 and KM56 were taken from cobbles in a conglomerate of the Upper Jurassic series (Tithonian and Oxfordian, Fig. 3c). The ChRM directions are defined between 550 and 650 °C, and median destructive fields are high (>20 mT; Figs 10a and c). The statistical analysis is determined with the Watson (1956) test, which yielded: $N = 10$, $R = 9.4$, $R_0 = 5.1$, and $N = 9$, $R = 8.6$, $R_0 = 4.84$ for sites KM31 and KM56, respectively. In both cases, the R values are higher then the critical R_0 value, therefore the rejection of the null hypothesis of randomness is verified (Figs 10b and d). Conversely, the conglomerate test from Valanginian–Hauterivian (A. M. Nikishin, personal communication) limestone cobbles defined by directional components isolated at high unblocking temperature or high coercivity from site KM70 (Figs 3c and 10e) shows a random distribution: $N = 10$, $R = 5.04$, $R_0 = 5.1$, which defines a positive conglomerate test, although it was not possible to take samples from the host rock to perform a full conglomerate test (Fig. 10f).

In a narrow region around Feodosiya, which lies in the easternmost part of Crimea (Fig. 2c), sandstone samples from sites KM74, KM76–79 show a mean direction of $D/I = 2.4^\circ/49.7^\circ$ ($k = 29.9$, $\alpha_{95} = 14.2^\circ$) and $D/I = 71.4^\circ/63.1^\circ$ ($k = 68.1$, $\alpha_{95} = 9.3^\circ$), before and after tilt corrections, respectively (Table 1, Fig. 8d). The mean direction shows best grouping of ChRM directions after 64.2 per cent untilting using Watson & Enkin (1993) (see Fig. 9; CUJ/Feodosiya), however, the grouping is significant at 0 and 100 per cent corrections (Table 1, Fig. 8d). Although the fold test is inconclusive a positive conglomerate test at site KM75 ($N = 10$, $R = 5.0$, $R_0 = 5.1$; Figs 10g and h), in which ChRM directions are obtained from high unblocking temperature and high coercive components (Figs 10g and h), suggests that the magnetization is primary. The age of the sandstones and cobbles used in this study was dated as Tithonian, according to the foraminifera determined on carbonate clay samples (Kuznetsova & Gorbachik 1985; Guzhikov *et al.* 2012). Primary magnetization from Tithonian sediments around Feodosiya were also reported in the study of Guzhikov *et al.* (2012). The authors found palaeomagnetic directions of mixed polarity with counter-clockwise rotations and significantly lower inclination then sites KM74–79. Because of the complex structures in this region that could be combined with our field observations, we attributed the large rotations to regional events, involving many faults and thrusts.

4.2.2 Pontides

Palaeomagnetic directions from the Triassic–Lower Jurassic rocks in the Central Pontides either demagnetized quickly or were unstable on demagnetization so that magnetic components or sites yielded mean directions with $\alpha_{95} > 20^\circ$ (PO25, PO31); these sites were excluded from further interpretation. Eight reliable sites were obtained from Barremian to Berriasian rocks (PO1–8) (Table 1), yielding a ChRM mean direction of $D/I = 341.0^\circ/53.3^\circ$ ($k = 25.7$, $\alpha_{95} = 11.1^\circ$) before tilt correction and $D/I = 332.5^\circ/35.6^\circ$ ($k = 6.5$, $\alpha_{95} = 23.5^\circ$) after tilt correction (Fig. 11a). The fold test of Watson & Enkin (1993) indicates an optimum clustering at 20.6 per cent with 95 per cent confidence limits at 26.3 and 14.0 per cent (Fig. 11c).

Upper Cretaceous sedimentary rocks from the Pontides carry a mean direction of $D/I = 320.1^\circ/36.0^\circ$ ($k = 18.5$, $\alpha_{95} = 11.5^\circ$) before tilt correction and $D/I = 323.4^\circ/46.9^\circ$ ($k = 34.0$, $\alpha_{95} = 10.5^\circ$) after tilt correction (Fig. 11b). To determine the timing and stability of the remanence, the fold test of Watson & Enkin (1993) indicates maximum unfolding at 83.7 per cent with confidence intervals at 75 and 92.0 per cent (Fig. 11c). We assume that the magnetization was acquired prior to folding.

Two conglomerate tests were performed at sites PO21 and PO22 (Fig. 12) on lava cobbles from two conglomerate beds of the Upper Cretaceous Yemişliçay Formation. The ChRM directions for both sites are defined between 500 and 650 °C (e.g. PO21.9 and PO22.5, Figs 12a and c, respectively). The isolated ChRM directions of individual volcanic cobbles are shown in Figs 12(b) and (d). The samples from sites PO21 and PO22 show a random distribution at the 95 per cent confidence level according to the Watson test: $N = 10$, $R = 4.94$, $R_0 = 5.1$ and $N = 9$, $R = 4.81$ $R_0 = 4.84$, respectively, suggesting that the ChRM of the Upper Cretacous Yemişliçay Formation have been stable since deposition of the conglomerates and has not been remagnetized.

5 DISCUSSION

5.1 Age and timing of magnetization and comparison of palaeomagnetic poles

5.1.1 Crimea

The palaeomagnetic results from the Triassic to Upper Jurassic clastic and carbonate sediments in Crimea indicate that almost all sites

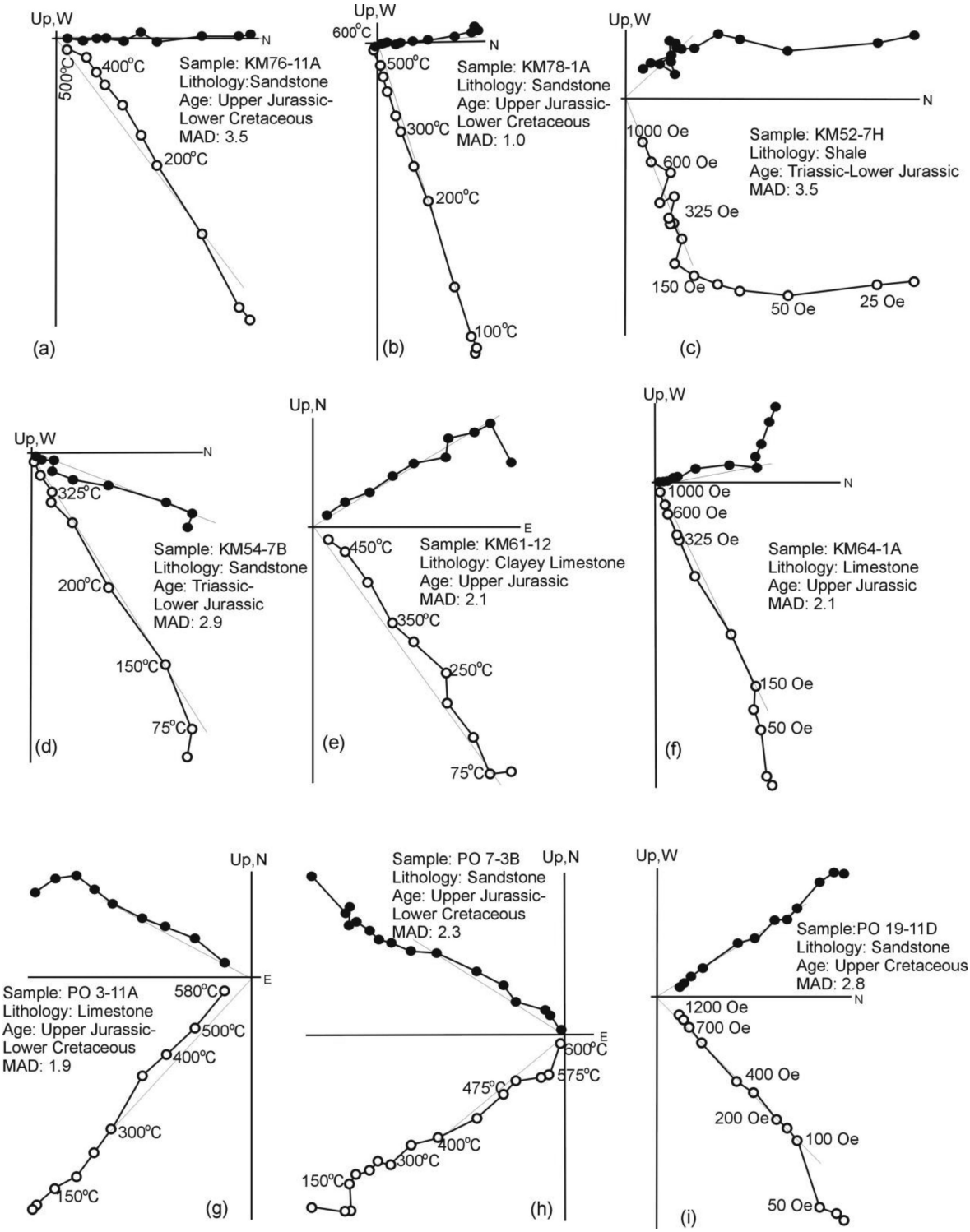

Figure 7. Zijderveld diagrams of representative samples during stepwise thermal and alternating field demagnetization (in degrees Celsius and mT). Solid (open) symbols for horizontal (vertical), respectively. A single component of magnetization is present after removal of a viscous component in almost all samples. Two components of magnetization are found in some sites shown in sample KM52–7h, the low-temperature component is consistent with the present-day GAD field in the Crimea.

with few exceptions have been remagnetized. This interpretation is supported by a negative conglomerate test in the Upper Jurassic and failed fold tests in Triassic to Upper Jurassic rocks. The positive conglomerate test in Valanginian–Hauterivian rocks (site KM70), however, indicates that the age of remagnetization must have occurred after deposition of the Upper Jurassic conglomerate and limestones, but before deposition of the Lower Cretaceous conglomerate.

The deformation that occurred after the remagnetization event in Crimea shows Upper Cretaceous to Pliocene stratigraphic sequence,

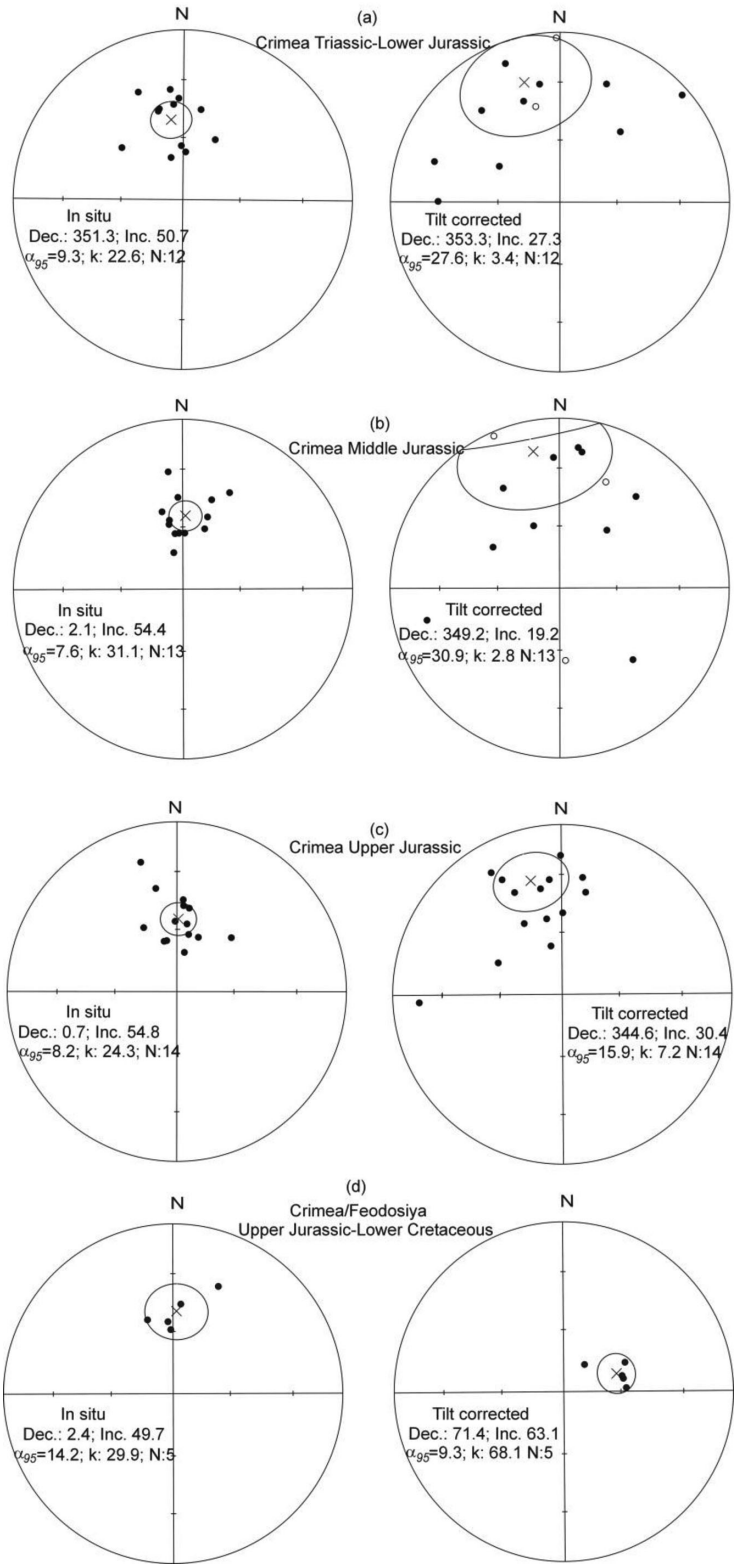

Figure 8. Equal-area stereographic projections showing the site mean directions of (a) Triassic–Lower Jurassic sites (b) Middle Jurassic sites, (c) Upper Jurassic sites, sites in Crimea before and after tilt corrections. Mean palaeomagnetic directions for each site are shown with 95 per cent confidence. Solid (open) symbols on lower (upper) hemisphere.

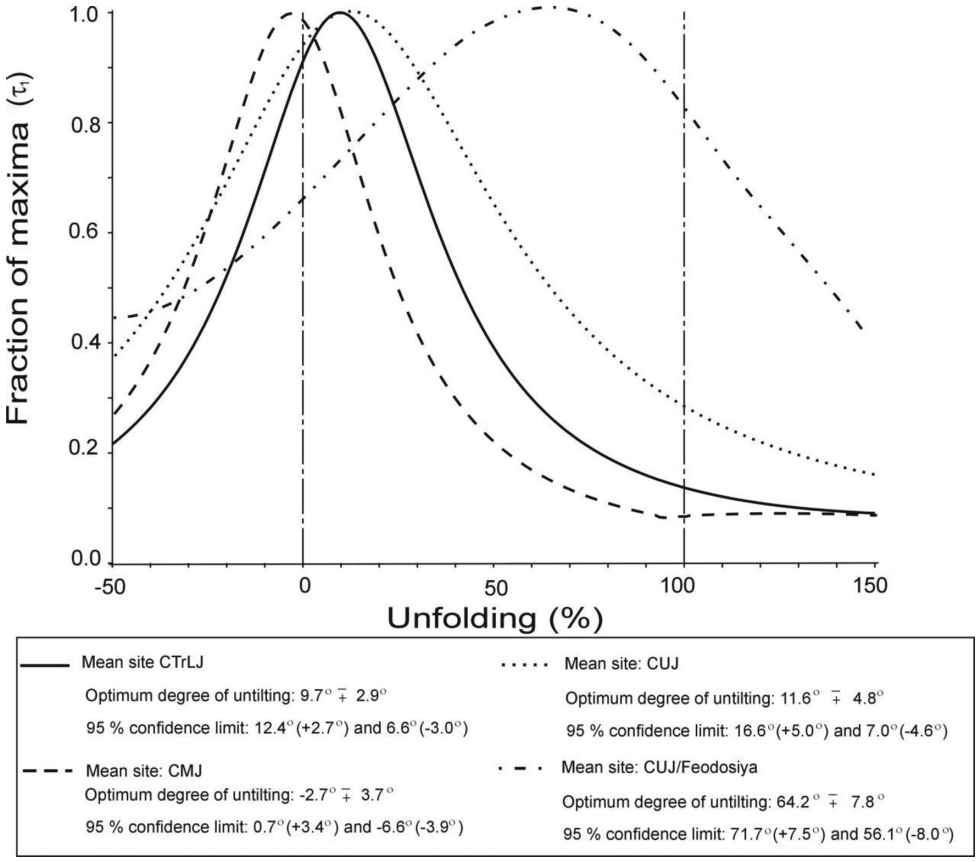

Figure 9. Results of stepwise unfolding of TLJ_1, CLJ and CUJ group means.

which is folded into a gentle anticline that is gently plunging to the northwest by 7°/323°. If we correct the mean ChRM directions of the remagnetized sites for this late-stage deformation there is only a slight shallowing in inclination by about 3°–5°, and no major change in declination. The change in inclination suggests that the entire region could have undergone N–S shortening equivalent to 2–5° latitude after the remagnetization.

The palaeomagnetic pole position calculated after the late-stage tilt correction of 7°/323° to the *in situ* data is 73.1°N, 218.8°E ($dp = 8.4$, $dm = 12.5$, $\alpha_{95} = 9.67°$) for CTrLJ age. Similarly, the remagnetized palaeomagnetic poles for the CMJ and Upper Jurassic CUJ are at 74.0°N, 184.6°E ($dp = 6.8$, $dm = 9.3$, $\alpha_{95} = 8.22°$) and 74.8°N, 187.4°E ($dp = 5.8$, $dm = 8.4$, $\alpha_{95} = 9.02°$), respectively (Table 2).

To better determine the age of remagnetization of Crimea, palaeomagnetic poles from Eurasia covering a time span between 200 Ma and the present (Torsvik *et al.* 2008; Table 2) are compared to the calculated palaeopole position of Crimea (Lat. = 45°N, Long. = 33°E) for three different time intervals (CTrLJ, CMJ and CUJ; Table 2). The discrepancy between the observed poles (λ_{obs}, ϕ_{obs}) and reference poles (λ_{ref}, ϕ_{ref}) are computed using the pole-space method of Beck (1980) to define the amount of the vertical-axis rotation (R), and poleward transport (p). The confidence limits ΔR and ΔF have been determined after Demarest (1983).

The lowest angular distance between the measured and reference values are $R \pm \Delta R = 5.9 \pm 7.2°$ and $F \pm \Delta F = 0.1 \pm 8.4°$ in CTrLJ; $R \pm \Delta R = 3.0 \pm 7.4°$ and $F \pm \Delta F = 0.4 \pm 6.4°$ in CMJ and $R \pm \Delta R = 1.9 \pm 8.1°$ and $F \pm \Delta F = -0.2 \pm 7.0°$ in CUJ for declination and inclination, respectively. This coincides with a time interval between the Aptian and Valanginian (110–140 Ma; Table 2).

The age of magnetization is an important point for the interpretation of these data and the following observations are noted below. Two sites (KM31 and KM56), which are taken from conglomerate deposits are Upper Jurassic (Tithonian and Oxfordian) in age and the results from the conglomerate tests are negative. Sites KM70 and KM75 also used in conglomerate tests were taken from different locations, one in the NW part of Crimea and the other around Feodosiya, in the eastern part of Crimea and yield positive conglomerate tests. It has been reported that the age of the coarse clastics at site KM70 is Valanginian–Hauterivian (A. M. Nikishin, personal communication), whereas the conglomerates around Feodesiya (site KM75 are Tithonian in age based on fossil evidence (Kuznetsova & Gorbachik 1985; Guzhikov *et al.* 2012). The difference between the ages of the conglomerates of sites KM70 and KM75 indicates that whereas remagnetization occurred during Lower Cretaceous in western Crimea, no remagnetization is recognized in the southeastern part of Crimea.

To constrain the age of magnetization, it is also necessary to consider the following arguments:

The ChRM directions show normal polarity in all three time intervals, which is compatible with the Cretaceous normal polarity superchron (Cande & Kent 1995). Therefore, it is more feasible to conclude that the age of magnetization is post-Berriasian. If we assume an age of magnetization during Lower Cretaceous times, it is necessary to consider the importance of the deformation history after Cretaceous which is associated with an N–S extension and NW–SE extension in the western Crimea during Oligocene (Saintot & Angelier 2002) and ending with the Alpine deformation, which

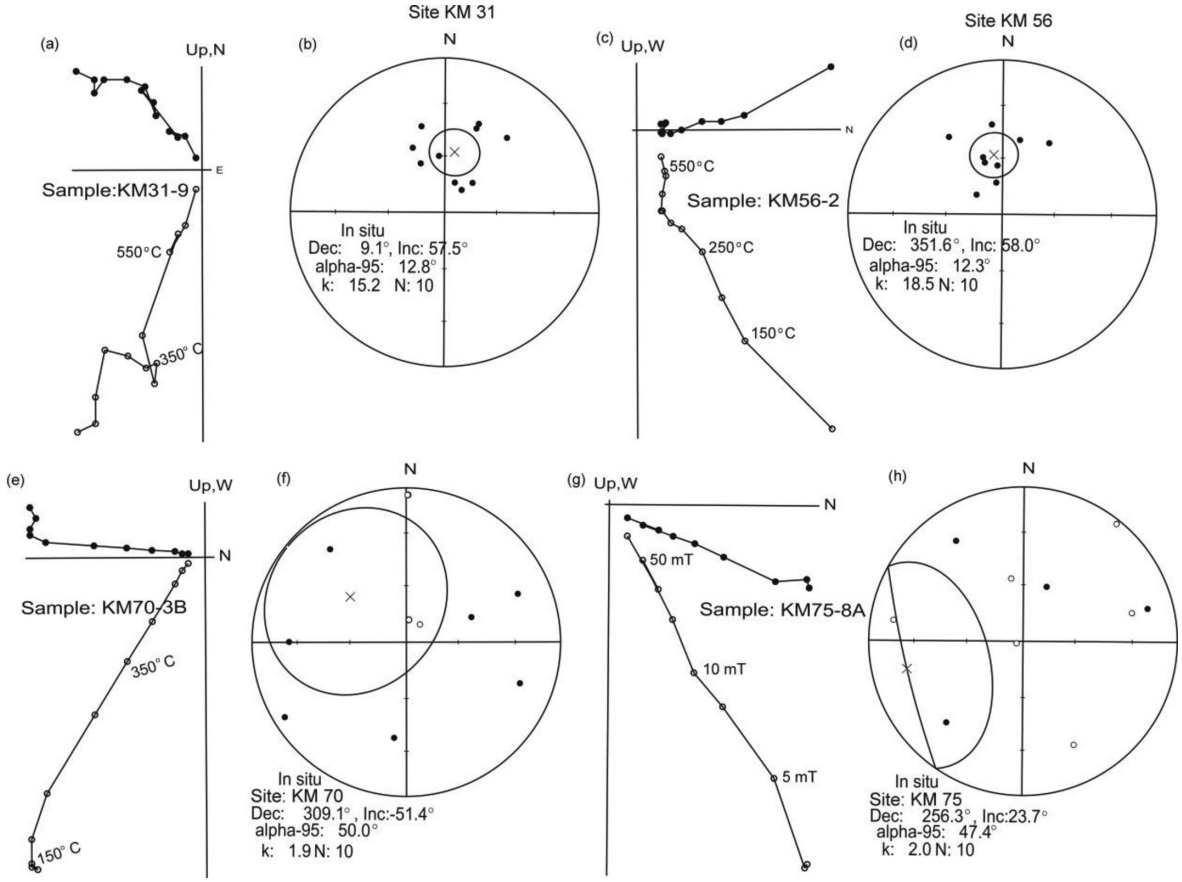

Figure 10. Typical Zijderveld diagrams of conglomerate samples from sites (a) KM31, (c) KM56, (e) KM70 and (g) KM75 showing the existence of a high-temperature component with an unblocking temperature of 660–690 °C. Directional distribution of block samples for conglomerate test with the statistical parameters (b, d, f and h).

produced S to SSE-vergent thrusting in the offshore part of Crimea (McKenzie 1972; Nowroozi 1972). As discussed earlier, this young deformation phase causes a gentle tilting to form a monocline that has a shallow dip. Accounting for this gentle tilt does not alter our interpretation that the Lower Cretaceous rocks in Crimea have undergone remagnetization. The palaeomagnetic results together with the positive conglomerate tests and the tectonic implications indicate that the magnetization in Crimea occurred in post-Berriasian, whereas the area around Feodesiya shows no remagnetization in the Tithonian. This is further supported by the results of Guzhikov *et al.* (2012).

5.1.2 Pontides

No stable palaeomagnetic directions were obtained from Triassic–Jurassic rocks in the Central Pontides. The Upper Jurassic–Lower Cretaceous rocks in the Western Pontides carry reliable palaeomagnetic directions but declinations are scattered to the northeast after tilt correction. The fold test of Watson and Enkin shows that the best statistical grouping is obtained at 20.6 per cent unfolding, therefore these sites could be remagnetizated, although further data should be acquired to confirm this result. The pole position is calculated from the 20.6 per cent of unfolding, because the difference between the best grouping mean and 20.6 per cent of unfolding directions is not statistically significant at the 95 per cent level of confidence. The pole position for the Pontides (PLC) is 70.5°N, 278.6°E ($\alpha_{95} = 10.7°$) (Table 2). A comparison between the calculated pole and the reference pole for Eurasia in the Lower Cretaceous (110 Ma) calculated after Torsvik *et al.* (2008) and Besse & Courtillot (2002, 2003) for a location in the Western Pontides (41°N, 32°E), has an angular distance of $R \pm \Delta R = 26.0 \pm 10.1°$ and $F \pm \Delta F = 1.2 \pm 8.3°$ (Table 2). No significant north–south displacement has occurred between the expected palaeolatitudes and the reference palaeolatitude, but significant tectonic rotation about vertical axes due to regional deformation since the Lower Cretaceous in the Pontides is recognized (Channell *et al.* 1996; Çinku *et al.* 2010; Meijers *et al.* 2010b).

The Late Cretaceous sites from the Pontides retain a primary magnetization on the basis of a positive conglomerate test which is further supported by a fold test at 100 per cent unfolding. An angular distance of $R = 37.6 \pm 9.5°$ and $F = 3.2 \pm 8.3°$, is obtained from a comparison of the calculated pole (58.0°N, 290.4°E, dp = 14.7, dm = 23.0, $\alpha_{95} = 10.9°$), and the Eurasian pole (80.3°N, 181.8°E, $\alpha_{95} = 2.7°$) in the Upper Cretaceous (PUC). The results support the conclusion that the Western Pontides had a palaeolatitude of ∼28°N in the Upper Cretaceous, consistent with previous palaeomagnetic results from this time period (Sarıbudak 1989a,b; Channell *et al.* 1996; Meijers *et al.* 2010b).

5.2 Tectonic implications

The palaeolatitudinal results from both the Pontides and Crimea are shown together in Fig. 13 with the Eurasian and Gondwana reference curves calculated for a location in Crimea (45°N, 33°E)

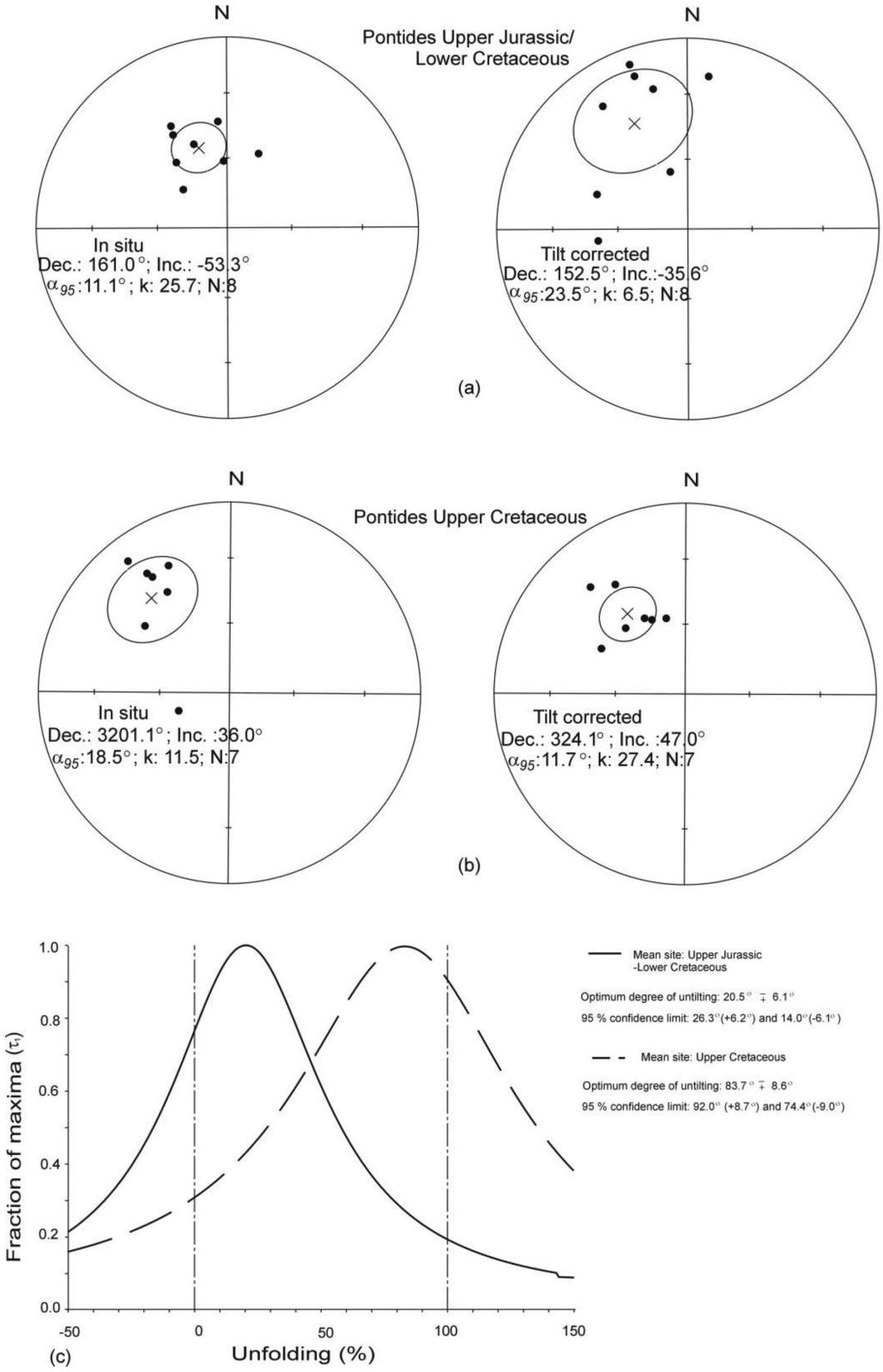

Figure 11. Equal-area stereographic projections showing the site mean directions of (a) Lower Cretaceous (b) Upper Cretaceous sites in the Western Pontides. (c) Results of stepwise unfolding of Upper Jurassic–Lower Cretaceous and Upper Cretaceous group means.

as a function of time using the GMAP 2003 software of Torsvik. The average palaeolatitudes calculated from *in situ* data of Crimea lie between 31 and 36.5°N, which is within error limits of the expected Lower Cretaceous palaeolatitude for this margin of Eurasia. Meijers *et al.* (2010a) reported Upper Jurassic palaeolatitudes in Crimea between 14 and 18.5°N for three sites (red solid circles KO, KV and UJ) and 31.6°N at a further site (red solid circle; site KA) after tilt correction. The authors considered the magnetization as

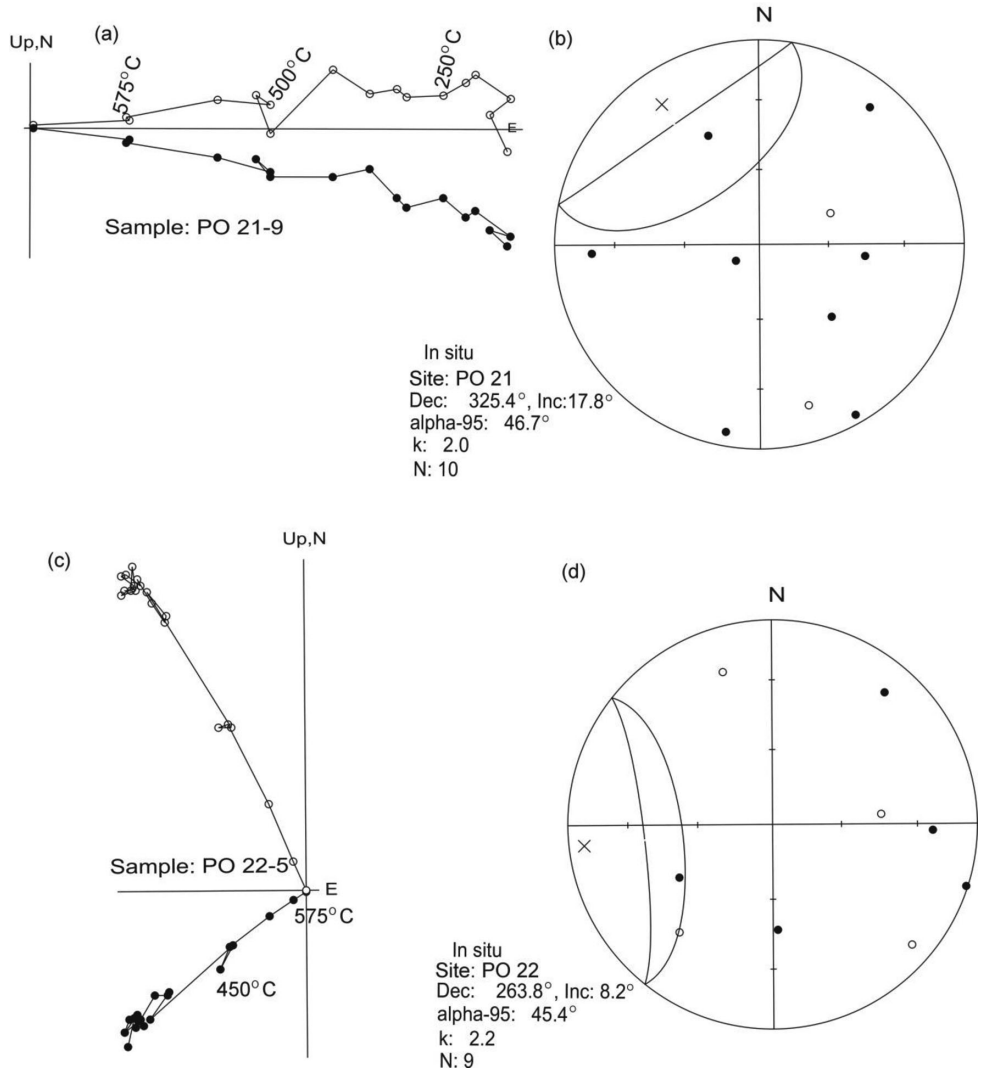

Figure 12. Typical Zijderveld diagrams of conglomerate samples from sites (a) PO and (c) PO showing the existence of high-temperature component with an unblocking temperature of 660–690 °C. (b and d) Directional distribution of block samples for conglomerate test with the statistical parameters.

primary. However, if we consider that their sites are also likely to be remagnetized, one can see that *in situ* data from sites KO and KV (Fig. 13, red solid squares) indicate the same palaeolatitude range as that obtained from this study, and site KA is within the error limits. Site KP with an age of 113 Ma, which has a palaeolatitude of ∼40°N is also consistent with our results. The Upper Jurassic rocks from site UJ of Meijers *et al.* (2010a), however, show a palaeolatitude of 10 and 18.5°N before and after tilt corrections, respectively, which is inconsistent with our results.

The Upper Jurassic–Lower Cretaceous mean direction from the Western Pontides shows a negative fold test and therefore indicates widespread remagnetization. We used the ChRM directions calculated from 20.6 per cent of untilting which yield a palaeolatitude of 31.2°N. Meijers *et al.* (2010a) reported on two sites (TD14 and TD2) with an age of 160 Ma, where one site has a mean palaeolatitude of 16°N and the other site a palaeolatitude of 26.4°N after tilt correction. Çinku (2011), however, found a mean palaeolatitude of $30.5^{\circ}\mathrm{N}^{+6.9}_{-5.8}$ for the eastern Pontides from Jurassic volcanoclastic rocks, and Channell *et al.* (1996) report a palaeolatitude of $41.5 \pm 4.5^{\circ}$ from the Pliensbachian Ammonitico Rosso facies. In addition, a mean palaeolatitude of 33.7°N was obtained from Upper Jurassic limestones in the Bilecik (Sakarya continent) by Evans *et al.* (1982). Hence, we consider that the Pontides and Crimea were in close proximity as suggested by geological evidence. The low palaeolatitudes derived from the Crimea (KV, KO and UJ) and Pontides (site TD14) by Meijers *et al.* (2010a) are therefore anomalous.

The remagnetized palaeomagnetic directions from Crimea in this study have a mean direction of $D/I = 357.8^{\circ}/52.8^{\circ}$ ($\alpha_{95} = 6.1^{\circ}$), which is consistent with the expected mean direction ($D/I = 3.9^{\circ}/53.2^{\circ}$) obtained from European pole in Lower Cretaceous (Besse & Courtillot 2002). After the remagnetization event Crimea moved in concordance with Eurasia, showing no significant rotation. One exception is a single region south of Feodosiya, in which palaeomagnetic results, which are assumed to carry a pre-folding magnetization reveal more than 70° CW rotation with respect to Eurasia. Such a large sense of rotation, however, is in contradiction with the main rotation phase of Crimea after remagnetization. The area also shows a higher inclination than those obtained for the whole of Crimea (Table 1). We conclude that this single region in the eastern part of Crimea is bounded by a left-lateral shear zone (Saintot *et al.* 1999) that could be the result of an internal tectonic deformation in the neotectonic regime.

In the Pontides, however, counter-clockwise rotations in Lower Cretaceous have also been found in previous studies (Sarıbudak

Table 2. Palaeomagnetic poles from Eurasia obtained for a time interval between 200 and 40 Myr, after Torsvik *et al.* (2008). The amount of the vertical-axis rotation (R) (positive indicates clockwise rotation), and poleward transport (p) (±, northwards/southwards) with their confidence limits ΔR and ΔF, after Demarest (1983), is calculated for each Crimean pole (TLJ_1, CLJ and CUJ) and the Pontides (LCP) relative to the Eurasian reference poles. The shaded area indicates the lowest angular difference between the considered pole and the reference pole.

Age (Ma)	Palaeopole of Eurasia			Palaeopole of Crimea TLJ_1 73.1°N, 218.8°E ($\alpha_{95} = 9.67$)		Palaeopole of Crimea CLJ 74.0°N, 184.8°E ($\alpha_{95} = 8.22$)		Palaeopole of Crimea CUJ 74.8°N, 187.4°E ($\alpha_{95} = 9.02$)		Palaeopole of the Pontides PLC 70.5°N, 278.6°E ($\alpha_{95} = 10.5$)	
	Lat. (°)	Long. (°)	α_{95} (°)	$R \pm \Delta R$ (°)	$I \pm \Delta I$ (°)	$R \pm \Delta R$ (°)	$I \pm \Delta I$ (°)	$R \pm \Delta R$ (°)	$I \pm \Delta I$ (°)	$R \pm \Delta R$ (°)	$I \pm \Delta I$ (°)
0	87.0	133.6	3.0	6.0 ± 8.6	16.1 ± 7.4	4.6 ± 7.7	13.8 ± 6.4	3.5 ± 8.3	13.3 ± 7.0	26.1 ± 10.1	9.3 ± 8.2
10	87.2	125.0	2.5	5.9 ± 8.5	16.6 ± 7.3	4.7 ± 7.5	14.3 ± 6.3	3.6 ± 8.1	13.8 ± 6.9	25.9 ± 9.9	9.7 ± 8.1
20	85.0	137.4	3.0	8.6 ± 8.6	15.3 ± 7.4	2.0 ± 7.6	13.0 ± 6.4	0.9 ± 8.3	12.5 ± 7.0	28.6 ± 10.1	8.4 ± 8.2
30	82.7	152.5	2.8	10.3 ± 8.5	12.9 ± 7.4	0.3 ± 7.5	10.6 ± 6.4	0.8 ± 8.2	10.0 ± 6.9	30.3 ± 10.0	5.9 ± 8.1
40	82.3	150.5	2.8	11.0 ± 8.5	12.8 ± 7.4	0.4 ± 7.5	10.5 ± 6.4	1.5 ± 8.2	10.0 ± 6.9	30.9 ± 10.0	5.9 ± 8.1
50	79.1	154.2	2.6	13.9 ± 8.4	10.5 ± 7.3	3.3 ± 7.4	8.2 ± 6.3	4.4 ± 8.1	7.6 ± 6.9	33.8 ± 9.9	3.5 ± 8.1
60	79.0	166.8	2.4	11.3 ± 8.3	8.7 ± 7.3	1.2 ± 7.3	6.4 ± 6.3	2.3 ± 8.0	5.9 ± 6.9	31.7 ± 9.8	1.8 ± 8.0
70	80.3	181.8	2.7	8.1 ± 8.4	8.3 ± 7.4	2.5 ± 7.4	6.0 ± 6.4	1.4 ± 8.1	5.4 ± 6.9	28.0 ± 9.9	1.4 ± 8.1
80	79.6	170.0	2.6	10.8 ± 8.4	8.8 ± 7.3	0.2 ± 7.4	6.5 ± 6.3	1.3 ± 8.1	6.0 ± 6.9	30.6 ± 9.9	1.9 ± 8.1
90	80.3	169.1	2.6	10.4 ± 8.4	9.4 ± 7.3	0.2 ± 7.4	7.1 ± 6.3	0.9 ± 8.1	6.6 ± 6.9	30.3 ± 9.9	2.5 ± 8.1
100	81.3	166.2	4.1	10.0 ± 8.9	10.5 ± 7.7	0.6 ± 8.0	8.2 ± 6.7	0.5 ± 8.6	7.7 ± 7.3	29.9 ± 10.3	3.6 ± 8.4
110	80.7	191.4	3.6	6.1 ± 8.7	6.1 ± 8.7	4.5 ± 7.7	5.7 ± 6.6	3.4 ± 8.4	5.2 ± 7.1	26.0 ± 10.1	1.2 ± 8.3
120	78.4	196.5	2.6	5.9 ± 7.2	5.6 ± 6.3	4.8 ± 7.4	3.3 ± 6.3	3.7 ± 8.1	2.7 ± 6.9	25.7 ± 9.9	−1.3 ± 8.1
130	75.2	193.6	2.9	7.67 ± 8.4	2.7 ± 7.4	3.0 ± 7.4	0.4 ± 6.4	1.9 ± 8.1	−0.2 ± 7.0	27.3 ± 9.9	−4.2 ± 8.1
140	70.4	176.7	6.1	15.0 ± 9.5	0.1 ± 8.4	4.3 ± 8.7	−2.2 ± 7.5	5.4 ± 9.2	−2.7 ± 8.0	34.7 ± 10.8	−6.8 ± 9.0
150	67.7	148.2	5.9	26.0 ± 9.6	4.5 ± 8.3	15.4 ± 8.7	2.2 ± 7.4	16.5 ± 9.3	1.6 ± 7.9	45.7 ± 10.9	−2.6 ± 9.0
160	68.2	136.2	6.0	28.7 ± 9.7	8.4 ± 8.4	18.1 ± 8.9	6.1 ± 7.5	19.2 ± 9.5	5.6 ± 8.0	48.5 ± 11.0	1.3 ± 9.0
170	69.9	126.1	3.8	28.8 ± 8.8	12.4 ± 7.6	18.2 ± 7.9	10.1 ± 6.6			48.7 ± 11.2	5.2 ± 9.0
180	68.8	116.7	3.6	31.6 ± 8.8	15.2 ± 7.6						
190	63.4	98.4	3.5	41.0 ± 9.0	21.6 ± 7.5						
200	59.2	102.3	3.2	46.9 ± 8.8	19.1 ± 7.5						

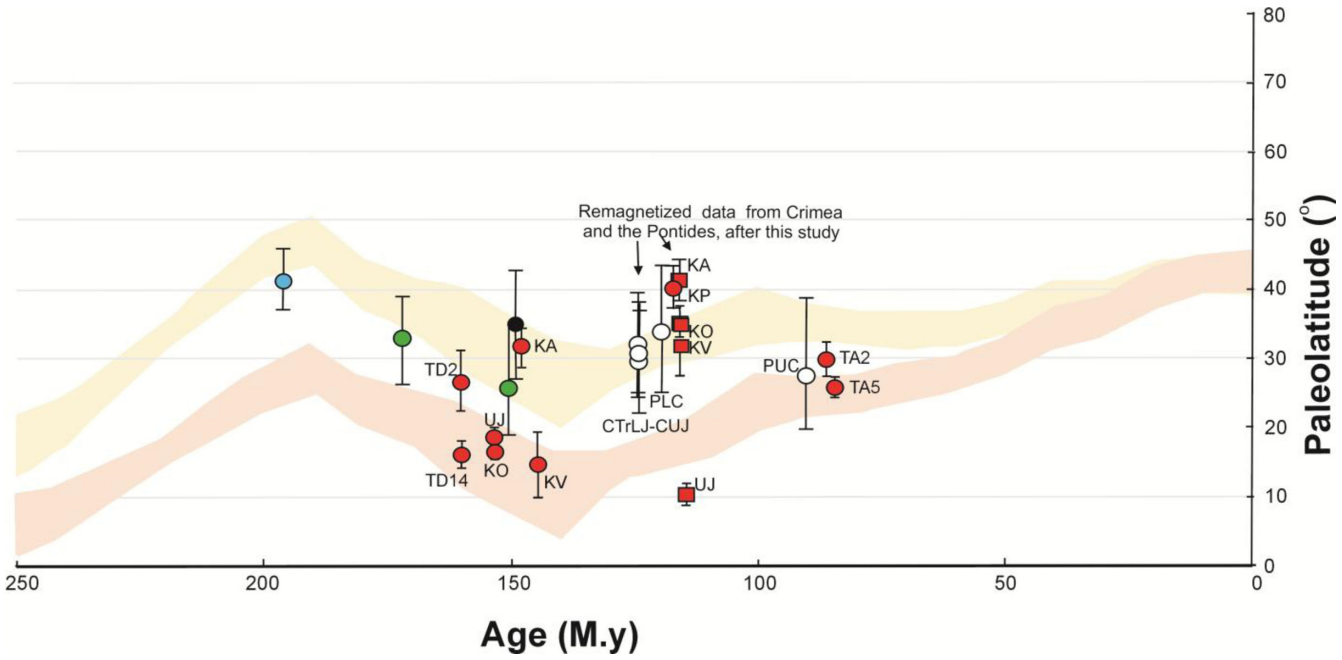

Figure 13. Age versus reference palaeolatitude curve with error envelopes derived from the APWP paths of Eurasia and Gondwana for a locality near Crimea (45°N, 33°E) after Torsvik *et al.* (2008). Previous palaeomagnetic data are taken from Channell *et al.* (1996) (blue circle), Evans *et al.* (1982) (black circle), Çinku (2011) (green circle), Meijers *et al.* (2010a) (red circles/tilt corrected, red squares/*in situ*) with error bars. Palaeomagnetic results from Crimea in this study are calculated from *in situ* data (hollow circles are drawn after this study).

1989a,b; Channell *et al.* 1996), suggesting that the Pontides experienced complex tectonic deformation after the rifting of the Black Sea. Meijers *et al.* (2010b) showed that different sense of rotations from Late Cretaceous sites in Central Pontides are consistent with the northward arc-shaped geometry of the Central Pontides that resulted from a oroclinal bending in latest Cretaceous to earliest Palaeocene times. The bending is interpreted to result from the closure of the Neotethys Ocean and the collision between the Pontides

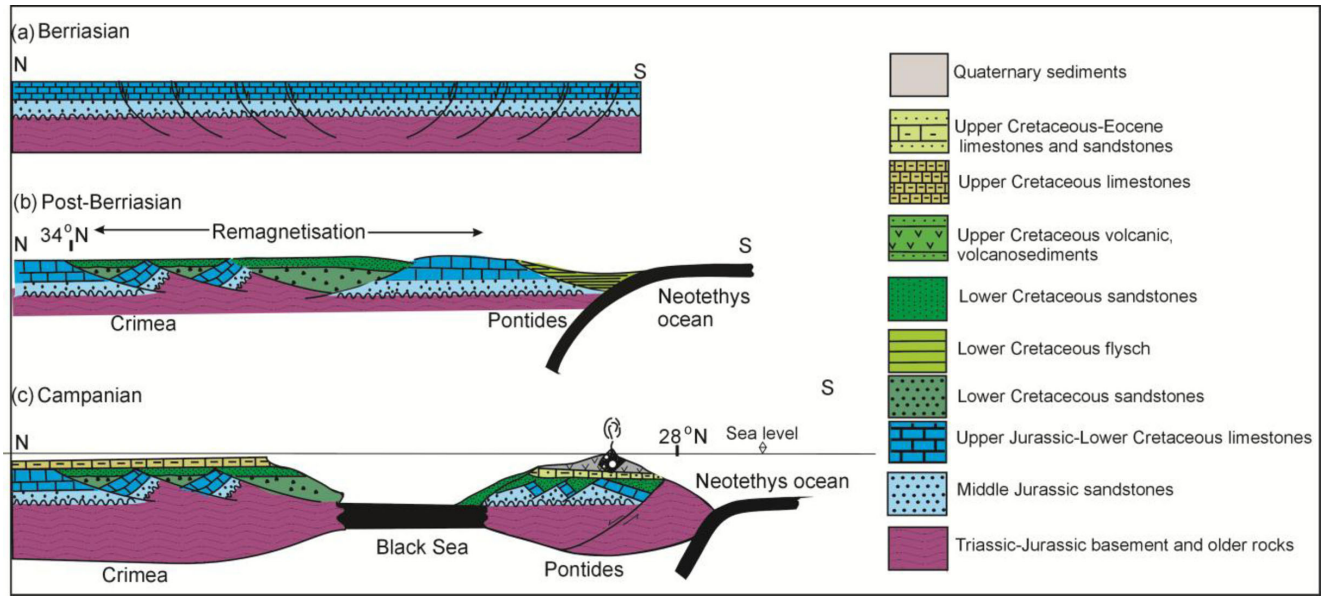

Figure 14. Summary of tectonic evolution of the Western Black Sea region during Upper Jurassic to Upper Cretaceous times. (a) A wide carbonate platform covered much of the whole present Black Sea area until Berriasian. (b) In the Lower Cretaceous, the breakup of the carbonate platform led to rifting of the Black Sea. In this stage, a widespread remagnetization occurred in Crimea. The palaeolatitude of the remagnetized rocks from Crimea placed the region to 34°N. (c) In Campanian, both the Pontides and Crimea separated by formation of the Western Black Sea Basin. At this stage, the stratigraphic evolution of the neighbouring regions changed.

and the Anatolide–Tauride Block. The Western Pontides are considered to be stable during the Eocene (Meijers *et al.* 2010b; Hisarli *et al.* 2011).

From geological observations, it is known that both the Pontides and Crimea were parts of a wide carbonate platform covering much of the present Black Sea region until the Berriasian, as the result of the collapse and erosion of the Kimmerian orogenic belt (Görür 1997; Görür & Tüysüz 1997; Ustaömer & Robertson 1997, Fig. 14a). The rifting of the Western Black Sea Basin led to the separation of the Pontides from the Crimea (Görür 1988, 1997; Yılmaz & Tüysüz 1988; Tüysüz *et al.* 1990; Görür *et al.* 1993; Okay *et al.* 1994; Fig. 14b). During this period, widespread remagnetization evidently occurred both in the Triassic–Lower Jurassic formations as well as during deposition of the Upper Jurassic limestones over almost the whole of Crimea. The palaeolatitude of the remagnetized rocks places the region at approximately 34°N. Later in the Upper Cretaceous, a new ocean basin, the Black Sea, formed between the Pontides and Crimea. At this stage, the stratigraphic evolution of the neighbouring regions changed; Upper Cretaceous–Eocene clayey limestones were deposited in the Crimea, whereas in the Pontides Upper Cretaceous magmatism influenced a wide area (Fig. 14c). During a later compressive phase, ophiolites were emplaced onto the Pontides, whereas in Crimea a shallow platform persisted. A palaeolatitude of 28°N obtained from this study in the Upper Cretaceous rocks in the Pontides indicates a southward movement of this block during the Lower to Upper Cretaceous interval.

We presently lack data to speculate on the origin of the widespread remagnetization in Crimea and the Western Pontides in the Lower Cretaceous. Remagnetization in orogenic belts has been often linked to fluid motion (e.g. Oliver 1986; Elmore *et al.* 2012) and orogenic fluids have been used to explain widespread remagnetization (e.g. Stamatakos *et al.* 1996; Enkin *et al.* 2000). This mechanism allows for the growth of new magnetic minerals such as magnetite in processes related to mineralization and dolomitization during folding. Our results show that buried remagnetized rocks, including Triassic–Lower Jurassic turbidites and Middle Jurassic sandstones and limestones, are considerably less magnetic than sandstones that are observed on the surface. If a thermoviscous magnetization is assumed, according to Dunlop *et al.* (2000), the rocks would have had to reach a palaeotemperature between 170 to 470 °C, based on their unblocking temperature in the laboratory. This suggests a buried depth down to ~6.5 km, which would have led to the rocks undergoing some degree of metamorphism. Because all lithologies from the Crimean sites show no metamorphism, the remagnetization cannot be explained by a thermoviscous origin. The origin of remagnetization may be chemical, but further geochemical information would be needed to verify this assumption.

6 CONCLUSION

A widespread remagnetization is found in Triassic to Late Jurassic limestones, sandstones and siltstones from the Crimean Peninsula. This is evident from the increased dispersion of mean directions after bedding correction, two negative conglomerate tests and statistical fold tests. The mean remagnetization directions are defined by a single stable component in most cases. Comparison of the average mean palaeomagnetic poles in the Triassic–Upper Jurassic units of Crimea with the expected Eurasian APWP, suggests an age of post-Berriasian.

In the Pontides, no reliable palaeomagnetic direction could be obtained from Triassic to Middle Jurassic sedimentary rocks. Remagnetization is also possible in the Upper Jurassic–Lower Cretaceous rocks from the Western Pontides as supported by a negative fold test. The timing of magnetization is considered to be Lower Cretaceous, consistent with the coeval Eurasian pole. The palaeolatitude obtained from *in situ* inclinations of the Upper Jurassic–Lower Cretaceous rocks is compatible with the Crimean Lower Cretaceous (~110–140 Ma) data. The Upper Cretaceous sites in the Pontides

show a palaeolatitude consistent with the expected palaeolatitude computed from stable Eurasia, whereas some tectonic rotations about vertical axes occurred in the Pontides after the opening of the Black Sea.

We conclude that regional remagnetization apparent from the palaeomagnetic results in Crimea until the Lower Cretaceous, and partly from the Upper Jurassic–Lower Cretaceous rocks in the Western Pontides, is related to the opening of the Black Sea Basin. This event is marked by a distinct unconformity in the stratigraphic section in both Crimea and the Pontides.

ACKNOWLEDGEMENTS

This study was financially supported by the joint project of the Scientific and Technical Research Council of Turkey (TUBITAK) and the National Academy Science of Ukraine (NASU) with project number 103Y151. The authors also thank for the financial assistance of the Scientific Research Projects Coordination Unit of Istanbul University (Project number UDP 13113). We would like to thank Sergei Yudin and Elena Yudina for their help in the field work. Victor Yudin is thanked very much for his helpful comments in the field. We thank to the Moskow University Field Camp government for the logistic support during our accommodation in Crimea. We dedicate this paper to the memory of our co-author Swetlana Kravchenko. Prof R. D. Elmore and anonymous reviewers are very much appreciated for their helpful suggestions.

REFERENCES

Abdüsselamoğlu, M.Ş., 1977. The Palaeozoic and Mesozoic in the Gebze region—explanatory text and excursion guidebook, in *4th Colloquium on the Aegean Region, Excursion 4,* İTÜ Maden Fak., İstanbul, 16pp.

Arkad'ev, V.V., Fedorova, A.A., Savel'eva, Yu.N. & Tesakova, E.M., 2006. Biostratigraphy of Jurassic-Cretaceous boundary sediments in the Eastern Crimea, *Stratigr. geol. Correl.,* **14**(3), 302–330.

Banks, C.J., 1997. Basins and thrust belts of the Balkan coast and the Black Sea, in *Regional and Petroleum Geology of the Black Sea and Surrounding Region,* pp. 115–128, ed. Robinson, A.G., AAPG Memoir 68.

Barka, A., 1992. The North Anatolian fault zone, *Ann. Tectonicae,* **6,** 164–195.

Beck, M.E., 1980. Paleomagnetic record of plate-margin tectonic processes along the western edge of North America, *J. geophys. Res.,* **85,** 7115–7131.

Besse, J. & Courtillot, V., 2002. Apparent and true wander and the geometry of the geomagnetic field over the last 200 Myr, *J. geophys. Res.,* **107**(B11), 2300, doi:10.1029/2000JB000050.

Besse, J. & Courtillot, V., 2003. Correction to "Apparent and true wander and the geometry of the geomagnetic field over the last 200 Myr", *J. geophys. Res.,* **108**(B10), 2469, doi:10.1029/2003JB002684.

Cande, S.C. & Kent, D.V., 1995. Revised calibration of the geomagnetic polarity timescale for the Late Cretaceous and Cenozoic, *J. geophys. Res.,* **100,** 6093–6095.

Cavazza, W., Okay, A.I. & Zattin, M., 2008. Rapid Early-Middle Miocene exhumation of the Kazdağ Massif, *Int. J. Earth. Sci.,* **98,** 1935–1947.

Channell, J.E.T., Tüysüz, O., Bektaş, O. & Şengör, A.M.C., 1996. Jurassic-Cretaceous paleomagnetism and paleogeography of the Pontides (Turkey), *Tectonics,* **15**(1), 201–212.

Çinku, M.C., 2011. Paleogeographic evidence on the Jurassic tectonic history of the Pontides: new paleomagnetic data from the Sakarya continent and Eastern Pontides, *Int. J. Earth. Sci.,* **100**(7), 1633–1645.

Çinku, M.C., Hirt, A.M., Hisarlı, Z.M., Heller, F. & Orbay, N., 2010. Southward migration of arc magmatism during latest Cretaceous associated with slab steepening, East Pontides, N Turkey: new paleomagnetic data from the Amasya region, *Phys. Earth planet. Inter.,* **182,** 18–29.

Day, R., Fuller, M. & Smith, V.A., 1977. Hysteresis properties of titanomagnetites, grain size and composition dependence, *Phys. Earth planet. Inter.,* **13,** 260–267.

Demarest, H.H., 1983. Error analysis for the determination of tectonic rotation from paleomagnetic data, *J. geophys. Res.,* **88,** 4321–4328.

Dercourt, J. *et al.*, 1986. Geological evolution of the Tethys belt from the Atlantic to the Pamirs since the Lias, *Tectonophysics,* **123,** 241–315.

Dercourt, J., Ricou, L.E. & Vrielynck, B. (Eds), 1993. *Atlas of Tethys Palaeoenvironmental Maps,* Gauthier-Villars, Paris, 307pp.

Dunlop, D.J., Özdemir, Ö., Clark, D.A. & Schmidt, P.W., 2000. Time temperature relations for the remagnetization of pyrrhotite (Fe7S8) and their use in estimating paleo-temperatures, *Earth planet. Sci. Lett.,* **176,** 107–116.

Dunlop, D.J., 2002. Theory and application of the Day plot (M_{rs}/M_s versus H_{cr}/H_c) 1. Theoretical curves and tests using titanomagnetite data, *J. geophys. Res.,* **107,** 2056, EPM 4-1–4-22.

Elmore, R.D., Muxworthy, A.R. & Aldana, M., 2012. Remagnetization and chemical alteration of sedimentary rocks, *Geol. Soc. Lond. Spec. Publ.,* **371,** doi:10.1144/SP371.15.

Enkin, R.J., Osadetz, K.G., Baker, J. & Kisilevsky, D., 2000. Orogenic remagnetizations in the front ranges and inner foothills of the southern Canadian Cordillera: chemical harbinger and thermal handmaiden of Cordilleran deformation, *Bull. geol. Soc. Am.,* **112**(6), 929–942.

Evans, I., Hall, S.A., Carman, M.F., Şenalp, M. & Coşkun, S.A., 1982. Paleomagnetic study of the Bilecik limestone (Jurassic), northwest Anatolia, *Earth planet. Sci. Lett.,* **61,** 199–208.

Finetti, I., Bricchi, G., Del Ben, A., Pipan, M. & Xuan, Z., 1988. Geophysical study of the Black Sea. *Boll. Geofis. Teor. Appl.,* **30**(117–118), 197–324.

Fisher, R.A., 1953. Dispersion on a sphere, *Proc. R. Soc. Lond.,* **A217,** 295–305.

Golonka, J., 2004. Plate tectonic evolution of the southern margin of Eurasia in the Mesozoic and Cenozoic, *Tectonophysics,* **381,** 235–273.

Görür, N., 1988. Timing and opening of the Black Sea basin, *Tectonophysics,* **147,** 47–262.

Görür, N., 1997. Cretaceous syn-to postrift sedimentation on the southern continental margin of the Western Black Sea Basin, in *Regional and Petroleum Geology of the Black Sea and Surrounding Region,* pp. 227–240, ed. Robinson, A.G., AAPG Memoir 68.

Görür, N. & Tüysüz, O., 1997. Petroleum geology of the southern continental margin of the Black Sea, in *Regional and Petroleum Geology of the Black Sea and Surrounding Region,* pp. 241–254, ed. Robinson, A.G., AAPG Memoir 68.

Görür, N., Tüysüz, O., Aykol, A., Sakınç, M., Yiğitbaş, E. & Akkök, R., 1993. Cretaceous red pelagic carbonates of northern Turkey—their place in the opening history of the Black Sea, *Eclogae geol. Helv.,* **86**(3), 819–838.

Guzhikov, A.Yu., Arkad'ev, V.V., Baraboshkin, E.Yu., Bagaeva, M.I., Piskunov, V.K., Rud'ko, S.V., Perminov, V.A. & Manikin, A.G., 2012. New sedimentological, bio-, and magnetostratigraphic data on the Jurassic–Cretaceous boundary interval of Eastern Crimea (Feodosiya), *Stratigr. geol. Correl.,* **20**(3), 261–294.

Hisarli, Z.M., Çinku, M.C. & Orbay, N., 2011. Paleomagnetic evidence of complex tectonic rotation pattern in the NW Anatolian region: implications for the tectonic history since the Middle Eocene, *Tectonophysics,* **505,** 86–99.

Kazantsev, Yu.V., 1982. *Tektonika Kryma (Tectonics of the Crimea),* Nauka, Moscow, 112pp.

Keskin, M., 2003. Magma generation by slab steepening and breakoff beneath a subduction accretion complex: an alternative model for collision-related volcanism in Eastern Anatolia, Turkey, *Geophys. Res. Lett.,* **30,** 8046, doi:10.1029/2003GL018019.

Keskin, M., Genç, Ş.C. & Tüysüz, O., 2008. Petrology and geochemistry of post-collisional Middle Eocene volcanic units in north-central Turkey: evidence for magma generation by slab breakoff following the closure of the northern Neotethys Ocean, *Lithos,* **104,** 267–305.

Keskin, S., Pedoja, K. & Bektaş, O., 2011. Coastal uplift along the Eastern Black Sea Coast: new marine tarrace data from eastern Pontides, Trabzon (Turkey) and a review, *J. Coast. Res.,* **27**(6A), 63–73.

Khain, V.Y., 1984. *Regionalnaya geotektonika. Alpiysko–Sredizemnomorskiy poyas, (Regional Geotectonics. The Alpine–Mediterranean Belt),* Nedra, Moscow, 344pp.

Kirschvink, J.L., 1980. The least-squares line and plane and the analysis of paleomagnetic data, *Geophys. J. R. astr. Soc.,* **62,** 699–718.

Koronovsky, N.V. & Mileyev, V.S., 1974. About the relationships of Tauric series and Eskiorda suite in the Bodrak river valley (Mountain Crimea), *Vestn. Mosk. Univ., Geologiya,* **1,** 80–87.

Kuznetsova, K.I. & Gorbachik, T.N., 1985. *Upper Jurassic and Lower Cretaceous Stratigraphy and Foraminiferas of the Crimea,* Nauka, Moscow, 136pp. (in Russian.)

Letouzey, J., Biju-Duval, B., Dorkel, A., Gonnard, R., Kristchev, K., Montadert, L. & Sungurlu, O., 1977. The Black Sea: a marginal basin; geophysical and geological data, in *International Symposium on the Structural History of the Mediterranean Basins,* pp. 363–376, eds Biju-Duval, B. & Montadert, L., Editions Technip, Paris.

Le Pichon, X. & Angelier, J., 1979. The Hellenic arc and trench system: a key to the neotectonic evolution of the eastern Mediterranean area, *Tectonophysics,* **60,** 1–42.

Lowrie, W., 1990. Identification of ferromagnetic minerals in a rock by coercivity and unblocking temperature properties, *Geophys. Res. Lett.,* **17,** 159–162.

Lysenko, N.I., 1976. New data about the Miocene planation surface in the Crimean Mountains [in Russian], *Geomorfol.,* **7,** 86–90.

McElhinny, M.W., 1964. Statistical significance of the fold test in paleomagnetism, *Geophys. J. R. astr. Soc.,* **8,** 338–340.

McFadden, P.L., 1990. The fold test as an analytical tool, *Geophys. J. Int.,* **135**(2), 329–338.

McKenzie, D.P., 1972. Active tectonics of the Mediterranean region, *Geophys. J. R. astr. Soc.,* **30,** 109–185.

Meijers, M.J.M., Langereis, C.G., van Hinsbergen, D.J.J., Kaymakcı, N., Stephenson, R.A. & Altıner, D., 2010a. Jurassic-Cretaceous low paleolatitudes from the circum-Black Sea region (Crimea and Pontides) due to True Polar Wander, *Earth planet. Sci. Lett.,* **296,** 210–226.

Meijers, M.J.M., Kaymakcı, N., van Hinsbergen, D.J.J., Langereis, C.G., Stephenson, R.A. & Hippolyte, J.-C., 2010b. Late Cretaceous to Paleocene oroclinal bending in the central Pontides (Turkey), *Tectonics,* **29,** TC4016, doi:10.1029/2009TC002620.

Mileyev, V.S., Baraboshkin, E.Y., Nikitin, M.Y., Rozanov, S.B. & Shalimov, I.V., 1996. Evidence that the Upper Jurassic deposits of the Crimean Mountains are allochtons, *Dokl. Earth Sci.,* **342**(4), 121–124.

Mileyev, V.S., Baraboshkin, E.Y., Rozanov, S.B. & Rogov, M.A., 2006. Cimmerian and Alpine tectonics of the Crimean Mountains, *Byull. Mosk. Obshch. Ispyt. Prir. Otd. Geol.,* **83,** 22–33.

Nikishin, A.M. *et al.*, 1996. Late Precambrian to Triassic history of the East European Craton: dynamics of sedimentary basin evolution, *Tectonophysics,* **268,** 23–63.

Nikishin, A.M., Cloetingh, S., Brunet, M.F., Stephenson, R.A., Bolotov, S.N. & Ershov, A.V., 1998. Scythian Platform, Caucasus and Black Sea region: Mesozoic-Cenozoic tectonic history and dynamics, in *Peri-Tethys Memoir 3: Stratigraphy and Evolution of Peri-Tethyan Platforms,* Vol. 177, pp. 163–176, eds Crasquin-Soleau, S. & Barrier, E., Mémoires du Muséum National d'Histoire Naturelle.

Nikishin, A.M., 2001. Mesozoic and Cenozoic evolution of the Scythian Platform Black Sea-Caucasus domain, in *Peri-Tethyan Rift/Wrench Basins and Passive Margins,* pp. 295–346, eds Ziegler, P., Cavazza, W., Robertson, A.H.F. & Crasquin-Soleau, S., Peri-Tethys Memoir, 5, Memoires du Museum National D'Histoire Naturelle, Paris.

Nikishin, A.M., Ziegler, P.A., Bolotov, S.N. & Fokin, P.A., 2011. Late Palaeozoic to Cenozoic evolution of the Black Sea-Southern Eastern Europe region: a view from the Russian Platform, *Turk. J. Earth Sci.,* **20,** 1–64.

Nowroozi, A.A., 1972. Focal mechanism of earthquakes in Persia, Turkey, West Pakistan, and Afghanistan and plate tectonics of the Middle East, *Bull. seism. Soc. Am.,* **62,** 823–850.

Okay, A.I. & Satır, M., 2006. Geochronology of Eocene plutonism and metamorphism in northeast Turkey: evidence for a possible magmatic arc, *Geodin. Acta,* **19,** 251–266.

Okay, A.İ., Şengör, A.M.C. & Görür, N., 1994. Kinematic history of the opening of the Black Sea and its effect on the surrounding regions, *GSA Bull.,* **22,** 267–270.

Okay, A.I., Bozkurt, E., Satır, M., Yiğitbaş, E., Crowley, Q.G. & Shang, C.K., 2008. Defining the southern margin of Avalonia in the Pontides: geochronological data from the Late Proterozoic and Ordovician granitoids from NW Turkey, *Tectonophysics,* **461,** 252–264.

Okay, N., Zack, T., Okay, A.I. & Barth, M., 2011. Sinistral transport along the Trans-European Suture Zone: detrital zircon-rutile geochronology and sandstone petrography from the Carboniferous flysch of the Pontides, *Geol. Mag.,* **148,** 380–403.

Oliver, J., 1986. Fluids expelled tectonically from orogenic belts: their role in hydrocarbon migration and other geologic phenomena, *Geology,* **14,** 99–102.

Panek, T., Danisik, M., Hradecky, J. & Frisch, W., 2009. Morpho-tectonic evolution of the Crimean mountains (Ukraine) as constrained by apatite fission track data, *TerraNova,* **21**(4), 271–278.

Robinson, A.G. & Kerusov, E., 1997. Stratigraphic and structural development of the Gulf of Odessa, Ukrainian Black Sea: implications for petroleum exploration, in *Regional and Petroleum Geology of the Black Sea and Surrounding Region,* pp. 369–380, ed. Robinson, A.G., AAPG Memoir 68.

Saintot, A. & Angelier, J., 2002. Tectonic paleostress fields and structural evolution of the NW-Caucasus fold-and-thrust belt from Late Cretaceous to Quaternary, *Tectonophysics,* **357,** 1–31.

Saintot, A., Angelier, J. & Chorowicz, J., 1999. Mechanical significance of structural patterns identified by remote sensing studies: a multiscale analysis of tectonic structures in Crimea, *Tectonophysics,* **313,** 187–218.

Saintot, A., Brunet, M.-F., Yakovlev, F., Sébrier, M., Stephenson, R., Ershov, A., Chalot-Prat, F. & McCann, R., 2006. The Mesozoic-Cenozoic tectonic evolution of the Greater Caucasus, in *European Lithosphere Dynamics,* Vol. 32, pp. 277–289, eds Gee, D. & Stephenson, R.A., Geological Society of London, London.

Sarıbudak, M., 1989a. New results and a paleomagnetic overview of the Pontides in Northern Turkey, *Geophys. J. Int.,* **99,** 521–531.

Sarıbudak, M., 1989b. A paleomagnetic approach to the origin of the Black Sea, *Geophys. J. Int.,* **99,** 247–251.

Şengör, A.M.C., 1984. The Cimmeride orogenic system and the tectonics of Eurasia, *GSA Bull. Spec. Pap.,* **195,** 1–82.

Şengör, A.M.C. & Yılmaz, Y., 1981. Tethyan evolution of Turkey: a plate tectonic approach, *Tectonophysics,* **75,** 181–241.

Slavin, V.I., 1989. Geological evolution of the Crimea in the Mesozoic, *Vestn. Mosk. Univ.,* **6,** 24–36.

Spiridonov, E.M., Fedorov, T.O. & Ryakhovskii, V.M., 1990. Magmatic rocks of the Mountainous Crimea (1), *Byull. MOIP. Otd. Geol.,* **65**(4), 119–134.

Stamatakos, J., Hirt, A.M. & Lowrie, W., 1996. The age and timing of folding in the central Appalachians from paleomagnetic results, *Bull. geol. Soc. Am.,* **108,** 815–829.

Stephenson, R. & Schellart, W.P., 2010. The Black Sea back-arc basin: insights to its origin from geodynamic models of modern analogue, in *Sedimentary Basin Tectonics from the Black Sea and Caucasus to the Arabian Platform,* Vol. 340, pp. 11–21, eds Sosson, M., Kaymakcı, N., Stephenson, R.A., Bergerat, F. & Starostenko, V., Geol. Soc. London Spec. Publ.

Sysolin, A.I. & Pravikova, N.V., 2008. Subvolcanic bodies of the Bodrak Complex in the Southwestern Crimea: structure, composition, and formation conditions, *Moscow Univ. Bull.,* **63**(2), 79–85.

Şengör, A.M.C., Yılmaz, Y. & Sungurlu, O., 1984. Tectonics of the Mediterranean Cimmerides: nature and evolution of the western termination of Palaeo-Tethys, in *The Geological Evolution of the Eastern Mediterranean,* Vol. **17,** pp. 77–112, eds Dixon, J.E. & Robertson, A.H.F., Geol. Soc. London Spec. Publ.

Şengör, A.M.C., Tüysüz, O., Imren, C., Sakınç, M., Eyidoğan, H., Görür, N., Le Pichon, X. & Rangin, C., 2005. The North Anatolian Fault: a new look, *Ann. Rev. Earth planet. Sci.,* **33,** 37–112.

Torsvik, T.H, Muller, R.D., Van der Voo, R., Steinberger, B. & Gaina, C., 2008. Global plate motion frames: toward a unified model, *Rev. Geophys.,* **46,** RG3004, doi:10.1029/2007RG000227.

Tüysüz, O., 1999. Geology of the Cretaceous sedimentary basins of the Western Pontides, *Geol. J.,* **34,** 75–93.

Tüysüz, O. & Dellaloglu, A.A., 1992. Çankırı havzasinin tektonik birlikleri ve havzanin tektonik evrimi, in *Proceedings of the Turk. Petrol. Congr., 9,* Turkey, Ankara, pp. 333–349.

Tüysüz, O., Yılmaz, Y., Yiğitbaş, E. & Serdar, H.S., 1990. Upper Jurassic–Lower Cretaceous stratigraphy of the central Pontides and its tectonic significance, in *Proceedings of 8th Int. Pet. Eng. Congress Turkey,* Turkish Association of Petroleum Geologists – UCTEA Chamber of Petroleum Engineers, pp. 340–351 (in Turkish with English abstract).

Tüysüz, O., Dellaloglu, A.A. & Terzioglu, N., 1995. A magmatic belt within the Neo-Tethyan suture zone and its role in the tectonic evolution of northern Turkey, *Tectonophysics,* **243,** 173–191.

Tüysüz, O., Yılmaz, İ.Ö., Švábenická, L. & Kirici, S., 2012. The Unaz Formation: a key unit in the Western Black Sea region, N Turkey, *Turk. J. Earth Sci.,* **21,** 1009–1028.

Ustaömer, P.A., Ustaömer, T., Gerdes, A. & Zulauf, G., 2011. Detrital zircon ages from a Lower Ordovician quartzite of the İstanbul exotic terrane (NW Turkey): evidence for Amazonian affinity, *Int. J. Earth Sci.,* **100**(1), 23–41.

Ustaömer, T. & Robertson, A.H.F., 1993. Late Paleozoic–Early Mesozoic marginal basins along the active southern continental margin of Eurasia: evidence from the Central Pontides (Turkey) and adjacent regions, *Geol. J.,* **28,** 219–238.

Ustaömer, T. & Robertson, A.H.F., 1994. Late Palaeozoic marginal basin and subduction-accretion: evidence from the Palaeotethyan Küre Complex, Central Pontides, N Turkey, *J. geol. Soc. Lond.,* **151,** 291–306.

Ustaömer, T. & Robertson, A.H.F., 1997. Tectonic sedimentary evolution of the North Tethyan margin in the Central Pontides of Northern Turkey, in *Regional and Petroleum Geology of the Black Sea and Surrounding Region,* pp. 255–290, ed. Robinson, A.G., AAPG Memoir 68.

Ustaömer, T. & Robertson, A.H.F., 2010. Late Palaeozoic–Early Cenozoic tectonic development of the Eastern Pontides (Artvin area), Turkey: stages of closure of Tethys along the southern margin of Eurasia, in *Sedimentary Basin Tectonics from the Black Sea and Caucasus to the Arabian Platform,* Vol. 340, pp. 281–327, eds Sosson, M., Kaymakci, N., Stephenson, R.A., Bergerat, F. & Starostenko, V., Geological Society, London, Special Publications.

Van der Voo, R., 1990. The reliability of paleomagnetic data, *Tectonophysics,* **184,** 1–9.

Watson, G.S., 1956. A test for randomness, *Mon. Not. R. astr. Soc.,* **7,** 160–161.

Watson, G.S. & Enkin, R.J., 1993. The fold test in paleomagnetism as a parameter-estimation problem, *Geophys. Res. Lett.,* **20,** 2135–2137.

Yergök, A.F. *et al.*, 1987a. Batı Karadeniz Bölgesinin Jeolojisi part I, MTA Report No. 8273, Ankara, unpublished.

Yergök, A.F. *et al.*, 1987b. The geology of Western Black Sea part II, MTA Report No. 8848, Ankara, unpublished.

Yılmaz, Y. & Tüysüz, O., 1988. An approach to the problem of reconstructing the Mesozoic tectonic units in the Kargı Massif and its surroundings, *Turk. Assoc. Petrol. Geol.,* **1**(1), 73–86 (in Turkish with English Abstract).

Yılmaz, Y., Genc, S.C., Yigitbas, E., Bozcu, M. & Yılmaz, K., 1995. Geological evolution of the Late Mesozoic continental margin of northwestern Anatolia, *Tectonophysics,* **243,** 155–171.

Yılmaz, Y., Tüysüz, O., Yiğitbaş, E., Genç, S.C. & Şengör, A.M.C., 1997. Geology and tectonic evolution of the Pontides, in *Regional and Petroleum Geology of the Black Sea and Surrounding Region,* pp. 183–226, ed. Robinson, A.G., AAPG Memoir 68.

Yudin, V.V., 1999. To the discussion about Crimean tectonics (in Russian), *Byull. Mosk. Obshch. Ispyt. Prir. Otd. Geol.,* **74,** 52–58.

Yudin, V.V., 2000. *Geology of Crimea (Based on Geodynamics),* Ural Branch, RAS, Syktyvkar, 42pp. (in Russian.)

Yudin, S.V., 2007. Paleomagnetic studies of the Middle Jurassic rocks from Crimea, *St. Petersburg Univ. Bull. Ser.,* **7**(1), 21–30.

Zijderveld, J.D.A., 1967. AC demagnetization of rocks: analysis of results, in *Methods in Paleomagnetism,* pp. 254–286, eds Collinson, D.W., Creer, K.M. & Runcorn, S.K., Elsevier, Amsterdam.

Zonenshain, L.P. & Le Pichon, X., 1986. Deep basins of the Black Sea and Caspian Sea as remnants of Mesozoic back-arc basins, *Tectonophysics,* **123,** 181–211.